であることが報告された[14]。そして，培養皿上で患者由来の皮膚線維芽細胞に，レンチウイルスベクターを用いて同疾患の原因遺伝子の野生型(正常型)を遺伝子導入し修復することによって，初めて iPS 細胞が樹立可能となることが示された。これは，Fanconi 貧血の原因遺伝子が，iPS 細胞の出現する過程であるリプログラミング現象，あるいは iPS 細胞の増殖に必須の役割を果たしている可能性を示唆する。今回，MPA 患者由来の線維芽細胞から iPS 細胞が樹立可能であったことより，MPA 発症に関与する遺伝的背景は，リプログラミングや iPS 細胞の増殖に必須の役割は果たしていないことが考えられた。

既報の分化誘導法を用いて，MPA 患者由来 iPS 細胞が同疾患の罹患臓器である血管に分化誘導可能であることが判明した。今後，本分化誘導系を用いて新規の試験管内疾患モデルの確立を目指す。最近，千葉大学の鈴木らの報告によると，myeloperoxidase(MPO)-ANCA 自己抗体が好中球に反応する以外に，血管内皮に発現する分子である moesin に作用することが示され，ANCA 抗体の血管への直接作用が同疾患の血管傷害メカニズムの一つである可能性が示された[15]。本研究において確立を目指す疾患モデルが，患者由来の血管内皮と MPO-ANCA 抗体の直接作用を検証する病態解析研究などに使用可能な新規のツールとなることが期待される。

おわりに

今後，MPA 患者由来 iPS 細胞から分化誘導された血管内皮を京都大学 iPS 細胞研究所にてすでに樹立されている健常日本人由来 iPS 細胞株から分化誘導された血管内皮と比較検討する。具体的には，形態学的特徴，分化誘導効率や増殖能を含めた細胞学的解析を行う。さらに，DNA マイクロアレイ，プロテインアレイを用いた遺伝子発現解析を行い，患者由来血管内皮にて特異的に発現する，あるいは，発現量が変化する分子を同定し，バイオマーカーの開発につなげる予定である。

また，MPA 患者由来 iPS 細胞から MPA 発症への関与が考えられている好中球やリンパ球など白血球への分化誘導も試みる。そして，MPA 患者由来 iPS 細胞から分化誘導した血管内皮と白血球との共培養を行い，両者の相互作用の機構を解析可能とする新規の試験管内疾患モデルの確立も併せて行う。

現在までに，多数の難治性疾患から疾患モデル作製目的にて iPS 細胞が樹立されているが，神経変性疾患，血液疾患，心疾患が多く，腎疾患の報告は存在しない。今後，iPS 細胞技術を用いた疾患モデル作製研究が難治性腎疾患にも適用され，新規の診断法や治療薬の開発に発展することが期待される。

謝　辞

本研究の遂行にあたり多くのご助言をいただきました千葉大学大学院医学研究院免疫発生学・炎症制御学教授　鈴木和男先生，血管分化誘導技術をご指導いただきました京都大学大学院医学研究科内分泌代謝内科学教授　中尾一和先生，曽根正勝先生，田浦大輔先生に深謝致します。また，本研究の一部は公益財団法人日本腎臓財団より研究助成の交付を受けて行われたものです。誌面をお借りして深く感謝申し上げます。

REFERENCES(参考文献)

1. Falk RJ, Jennette JC. Anti-neutrophil cytoplasmic autoantibodies with specificity for myeloperoxidase in patients with systemic vasculitis and idiopathic necrotizing and crescentic glomerulonephritis. N Engl J Med 1988；318：1651-7.
2. Jennette JC, Falk RJ. Small-vessel vasculitis. N Engl J Med 1997；337：1512-23.
3. Takahashi K, Yamanaka S. Induction of pluripotent stem cells from mouse embryonic and adult fibroblast cultures by defined factors. Cell 2006；126：663-76.
4. Takahashi K, Tanabe K, Ohnuki M, et al. Induction of pluripotent stem cells from adult human fibroblasts by defined factors.

Cell 2007 ; 131 : 861-72.
5. Yu J, Vodyanik MA, Smuga-Otto K, et al. Induced pluripotent stem cell lines derived from human somatic cells. Science 2007 ; 318 : 1917-20.
6. Saha K, Jaenisch R. Technical challenges in using human induced pluripotent stem cells to model disease. Cell Stem Cell 2009 ; 5 : 584-95.
7. Dimos JT, Rodolfa KT, Niakan KK, et al. Induced pluripotent stem cells generated from patients with ALS can be differentiated into motor neurons. Science 2008 ; 321 : 1218-21.
8. Park IH, Arora N, Huo H, et al. Disease-specific induced pluripotent stem cells. Cell 2008 ; 134 : 877-86.
9. Ebert AD, Yu J, Rose Jr FF, et al. Induced pluripotent stem cells from a spinal muscular atrophy patient. Nature 2009 ; 457 : 269-70.
10. Lee G, Papapetrou EP, Kim H, et al. Modelling pathogenesis and treatment of familial dysautonomia using patient-specific iPSCs. Nature 2009 ; 461 : 402-6.
11. Carvajal-Vergara X, Sevilla A, D' Souza SL, et al. Patient-specific induced pluripotent stem-cell-derived models of LEOPARD syndrome. Nature 2010 ; 465 : 808-12.
12. Taura D, Sone M, Homma K, et al. Induction and isolation of vascular cells from human induced pluripotent stem cells—brief report. Atheroscler Thromb Vasc Biol 2009 ; 29 : 1100-3.
13. Homma K, Sone M, Taura D, et al. Sirt1 plays an important role in mediating greater functionality of human ES iPS-derived vascular endothelial cells. Atherosclerosis 2010 ; 212 : 42-7.
14. Raya A, Rodriguez-Piza I, Guenechea G, et al. Disease-corrected haematopoietic progenitors from Fanconi anaemia induced pluripotent stem cells. Nature 2009 ; 460 : 53-9.
15. Nagao T, Suzuki K, Utsunomiya K, et al. Direct activation of glomerular endothelial cells by anti-moesin activity of anti-myeloperoxidase antibody. Nephrol Dial Transplant 2011 ; 26 : 2752-60.

Induction and Enhancement of Cardiac Cell Differentiation from Mouse and Human Induced Pluripotent Stem Cells with Cyclosporin-A

Masataka Fujiwara[1,2], Peishi Yan[1,3¤], Tomomi G. Otsuji[4,5], Genta Narazaki[1,6], Hideki Uosaki[1,6], Hiroyuki Fukushima[1,6], Koichiro Kuwahara[2], Masaki Harada[2], Hiroyuki Matsuda[7], Satoshi Matsuoka[7], Keisuke Okita[8], Kazutoshi Takahashi[8], Masato Nakagawa[8], Tadashi Ikeda[3], Ryuzo Sakata[3], Christine L. Mummery[9], Norio Nakatsuji[10,11], Shinya Yamanaka[8,12], Kazuwa Nakao[2], Jun K. Yamashita[1,6]*

1 Laboratory of Stem Cell Differentiation, Stem Cell Research Center, Institute for Frontier Medical Sciences, Kyoto University, Kyoto, Japan, **2** Department of Medicine and Clinical Science, Kyoto University Graduate School of Medicine, Kyoto, Japan, **3** Department of Cardiovascular Surgery, Kyoto University Graduate School of Medicine, Kyoto, Japan, **4** Stem Cell and Drug Discovery Institute, Kyoto Research Park, Kyoto, Japan, **5** Laboratory of Embryonic Stem Cell Research, Stem Cell Research Center, Institute for Frontier Medical Sciences, Kyoto University, Kyoto, Japan, **6** Department of Cell Growth and Differentiation, Center for iPS Cell Research and Application (CiRA), Kyoto University, Kyoto, Japan, **7** Department of Physiology and Biophysics, Kyoto University Graduate School of Medicine, Kyoto, Japan, **8** Department of Reprogramming Science, Center for iPS Cell Research and Application (CiRA), Kyoto University, Kyoto, Japan, **9** Department of Anatomy and Embryology, Leiden University Medical Centre, Leiden, the Netherlands, **10** Department of Development and Differentiation, Institute for Frontier Medical Sciences, Kyoto University, Kyoto, Japan, **11** Institute for Integrated Cell-Material Sciences (iCeMS), Kyoto University, Kyoto, Japan, **12** Gladstone Institute of Cardiovascular Disease, San Francisco, California, United States of America

Abstract

Induced pluripotent stem cells (iPSCs) are novel stem cells derived from adult mouse and human tissues by reprogramming. Elucidation of mechanisms and exploration of efficient methods for their differentiation to functional cardiomyocytes are essential for developing cardiac cell models and future regenerative therapies. We previously established a novel mouse embryonic stem cell (ESC) and iPSC differentiation system in which cardiovascular cells can be systematically induced from $Flk1^+$ common progenitor cells, and identified highly cardiogenic progenitors as $Flk1^+/CXCR4^+/VE\text{-}cadherin^-$ (FCV) cells. We have also reported that cyclosporin-A (CSA) drastically increases FCV progenitor and cardiomyocyte induction from mouse ESCs. Here, we combined these technologies and extended them to mouse and human iPSCs. Co-culture of purified mouse iPSC-derived $Flk1^+$ cells with OP9 stroma cells induced cardiomyocyte differentiation whilst addition of CSA to $Flk1^+$ cells dramatically increased both cardiomyocyte and FCV progenitor cell differentiation. Spontaneously beating colonies were obtained from human iPSCs by co-culture with END-2 visceral endoderm-like cells. Appearance of beating colonies from human iPSCs was increased approximately 4.3 times by addition of CSA at mesoderm stage. CSA-expanded human iPSC-derived cardiomyocytes showed various cardiac marker expressions, synchronized calcium transients, cardiomyocyte-like action potentials, pharmacological reactions, and ultra-structural features as cardiomyocytes. These results provide a technological basis to obtain functional cardiomyocytes from iPSCs.

Citation: Fujiwara M, Yan P, Otsuji TG, Narazaki G, Uosaki H, et al. (2011) Induction and Enhancement of Cardiac Cell Differentiation from Mouse and Human Induced Pluripotent Stem Cells with Cyclosporin-A. PLoS ONE 6(2): e16734. doi:10.1371/journal.pone.0016734

Editor: Felipe Prosper, Clinica Universidad de Navarra, Spain

Received November 1, 2010; **Accepted** December 24, 2010; **Published** February 22, 2011

Funding: This study was supported by grants from the Ministry of Education, Science, Sports and Culture of Japan, the Ministry of Health, Labour and Welfare, the New Energy and Industrial Development Organization (NEDO) of Japan, the Project for Realization of Regenerative Medicine. The funders had no role in study design, data collection and analysis, decision to publish, or preparation of the manuscript.

Competing Interests: The authors have declared that no competing interests exist.

* E-mail: juny@frontier.kyoto-u.ac.jp

¤ Current address: Cardiovascular Department, Dalian Municipal Central Hospital, Dalian, China

Introduction

Induced pluripotent stem cells (iPSCs) are novel pluripotent stem cells generated from adult tissues by reprogramming originally with transduction of a few defined transcription factors, such as Oct4, Sox2, Klf4, and c-myc [1], [2]. Establishment of iPSC lines from adult human tissue is facilitating development of cell transplantation-based regenerative strategies and establishment of patient-derived cells as disease models. Efficient differentiation and dissecting the differentiation mechanisms of target cells would significantly contribute to elucidate the pathophysiology of diseases and provide a platform for developing new therapeutic strategies for specific diseases through such as drug discovery [3], [4].

Cardiomyocytes are a major target of regenerative medicine. Although cardiomyocyte differentiation has been reported from various progenitor and adult cell sources (e.g. bone marrow, cardiac biopsies, adipose tissue, umbilical cord, mesenchymal cells, etc), overall, the efficiencies of functional cardiomyocyte appearance have been still variable (<1–5%) [5]. Pluripotent cells, embryonic stem cells (ESCs) and iPSCs have thus emerged as among the most promising stem cell sources for inducing

functional cardiomyocytes in vitro. Several induction and purification methods have been reported, starting with either mouse or human ESCs. These include stem cell aggregation in suspension and growth as embryoid bodies (EBs), co-culture with stroma cells, serum-free culture in differentiation medium, or hypoxic culture [6], [7], [8], [9], [10], [11]. Overall, the efficiency of cardiomycyte differentiation in human ESCs [6] should be still lower than in mouse ESCs [8], [11]. In view of the similarities between iPSCs and ESCs, most cardiomyocyte induction methods from iPSCs are based on those tried and tested in ESCs. Several groups have thus reported cardiomyocyte formation from mouse iPSCs using either EBs or stroma cell co-culture [12], [13], [14]. Recently, several reports on cardiomyocyte induction from human iPSCs appeared with based on EB formation though the efficiencies are still varied [15], [16], [17], [18], [19]. Other new methods robust in human iPSCs remain to be explored and maybe of particular value for preparation of transplantation cell sources as well as dissecting the differentiation mechanisms and drug discovery.

Previously, we developed a novel ESC differentiation system that recapitulates early cardiovascular development in vivo [8], [20], [21]. Flk1 (also known as vascular endothelial growth factor (VEGF) receptor-2) is the earliest differentiation marker for endothelial cells (ECs) and blood cells, and is a marker of lateral plate mesoderm [21], [22]. We induced Flk1$^+$ cells from ESCs, purified them by fluorescence-activated cell sorting (FACS), and re-cultured the purified cells. We succeeded in inducing the major cardiovascular cell types from the common Flk1$^+$ progenitor cells: vascular ECs, mural cells (pericytes and vascular smooth muscle cells) [20] and cardiomyocytes [8]. When purified Flk1$^+$ cells were cultured on mouse bone marrow-derived stromal cells, OP9 cells, spontaneously beating cardiomyocytes as well as ECs can be induced within 3–4 days (Flk-d3-4) even from a single cell. We, thus, demonstrated that ESC-derived Flk1$^+$ cells serve as cardiovascular progenitors [8], [20], [23], which was further supported with following several mouse and human studies [9], [24], [25], [26]. We also identified a Flk1$^+$/CXCR4$^+$/vascular endothelial cadherin$^-$ (FCV) population as highly cardiogenic progenitor cells among the progeny of Flk1$^+$ mesoderm cells at the single cell level [8]. That is, in an intermediate stage of ESC differentiation between Flk1$^+$ mesoderm cells and cardiomyocytes (Flk-d2), purified FCV population could efficiently give rise to cardiomyocytes from a single cell. The cardiogenic potential of FCV cells was 15–20 times higher than that of other cell populations among the Flk1$^+$ cell progeny. We further confirmed FCV cells can differentiate into cardiomyocytes in vivo through cell transplantation experiments [11]. FCV cells, which are detected just 1–2 days before the cardiomyocyte appearance, are so far the nearest upstream cardiac progenitors to cardiomyocytes. This system proved amenable to induce various cardiovascular cells systematically from ESCs, explore novel differentiation methods, and dissect the differentiation processes [23], [27], [28]. Indeed, we recently succeeded in demonstrating that an immunosuppressant, cyclosporin-A (CSA) showed a novel potent effect specifically on Flk1$^+$ mesoderm cells to induce a dramatic increase in FCV cardiac progenitor cells and cardiomyocytes with the use of this ESC differentiation system [11]. That is, when CSA was added to Flk1$^+$ cells co-cultured on OP9 cells, appearance of FCV progenitor cells and cardiomyocytes were increased by 10–20 times.

Recently, we were able to systematically induce cardiovascular cells from mouse iPSCs in a way almost identical to that using mouse ESCs [12]. Here, we combined our technologies in ESCs and iPSCs and showed that FCV cardiac progenitors and cardiomyocytes were efficiently expanded from mouse iPSCs by CSA treatment. Moreover, we extended the CSA method to human iPSCs and showed that CSA also successfully worked in human iPSC differentiation and efficiently enhanced the appearance of spontaneously beating cells. Human iPSC-derived cardiomyocytes showed expected molecular, structural and functional features of human cardiomyocytes. We, thus, succeeded in inducing and enhancing cardiac cell differentiation from both mouse and human iPSCs.

Methods

Antibodies

Monoclonal antibodies (MoAbs) for murine E-cadhein (ECCD2), murine Flk1 (AVAS12) were prepared and labeled in our laboratory as described previously [8], [21], [29]. MoAb for cardiac troponin-T (cTnT) (1:2000) was purchased from Neo-Markers (Fremont, CA). For staining human ESCs and iPSCs, another MoAb for cTnT (1:100) was from Santa Cruz Biotechnology (Santa Cruz, CA). MoAbs for murine and human α-actinin (1:800) was from Sigma (St Louis, Mo). MoAb of phycoerithrin (PE)-conjugated AVAS12 was purchased from eBioscience (San Diego, CA). MoAbs for biotinylated-CXCR4 was purchased from BD Pharmingen (San Diego, CA). Anti-HCN4 (1:200) and anti-Cav3.2 (1:200) antibodies were from Chemicon (Temecula, CA). Anti-Kir2.1 (1:200) and anti-connexin 43 (1:200) antibodies were from Alomone (Israel) and Invitrogen (Carlsbad, CA), respectively.

Reagents

Cyclosporin-A (a gift from Novartis Pharma) was dissolved in Dimethyl sulfoxide (DMSO) (Nacalai Tesque, Kyoto Japan) at 30 mg/mL. Dilution of 1–3 μg/mL were made in differentiation medium at the time of use. PKH67 fluorescent dye was purchased from Sigma (St. Louis, MO).

Mouse iPSC culture

A germline-competent mouse iPSC line, 20D-17, carrying Nanog promoter-driven GFP/IRES/puromycin resistant gene (Nanog-iPS cells), was maintained as previously described [30]. Briefly, iPSCs were maintained in Dulbecco's Modified Eagle Medium (DMEM) containing 15% FCS, non-essential amino acids, 1 mmol/L sodium pyruvate, 5.5 mmol/L 2-mercaptoethanol, 50 units/mL penicillin and 50 mg/mL streptomycin on feeder layers of mitomycin-C-treated mouse embryonic fibroblast (MEF) cells carrying stably incorporated puromycin-resistance gene. OP9 stroma cells were maintained as described [21].

Induction of mouse cardiomyocyte differentiation

Induction of Flk1$^+$ cells and sorting for Flk1$^+$ cells were performed as previously described [8], [12], [20]. Briefly, mouse iPSCs were first plated on to gelatin-coated dishes and cultured for 30 min to eliminate attached feeder cells, then, non-adherent cells were collected and induced to differentiation. Mouse iPSCs were cultured at a density of $1–2.5\times10^3$ cells/cm^2 in differentiation medium (DM)(alpha minimum essential medium (GIBCO, Grand Island, NY) supplemented with 10% fetal calf serum) on type IV collagen-coated dishes (Biocoat, Beckton Dickinson) or mitomycin C-treated confluent OP9 cell sheets (MMC-OP9) for 96–108 h. Cells were collected and selected by FACS to purify Flk1$^+$ cells. Flk1$^+$ cells were then plated on to MMC-OP9 at a density of $1–10\times10^3$ cells/cm^2 and cultured in differentiation medium to induce cardiac differentiation. CSA (1–3 μg/mL) was added to Flk1$^+$ cells on OP9 cells. Medium was replaced every 2 days.

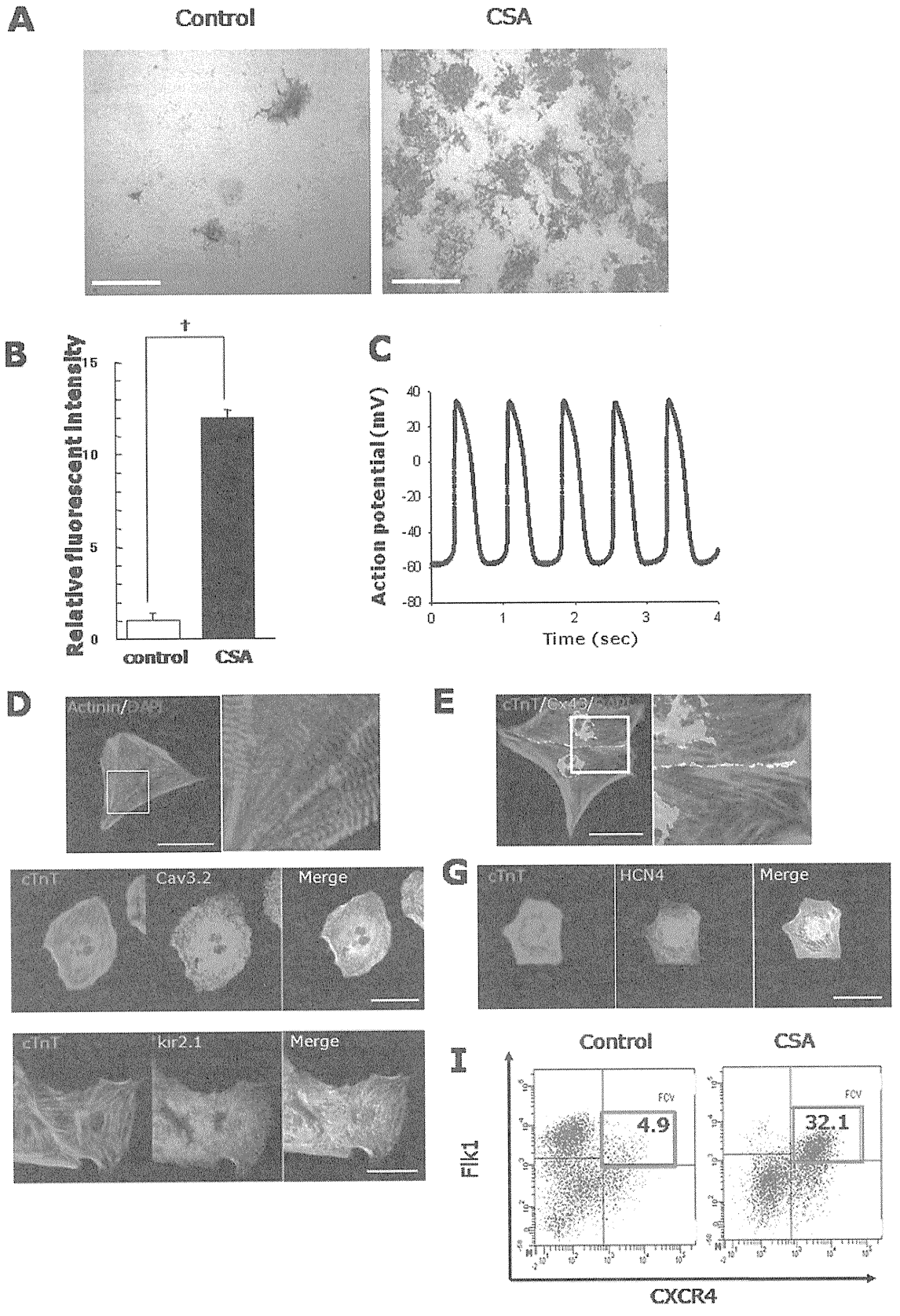

Figure 1. Cardiac cell expansion from mouse iPSC-derived Flk1$^+$ mesoderm by CSA. A. Gross appearance of cardiomyocyte induction by CSA. Six days after the Flk1$^+$ cell culture on OP9 cells (Flk-d6). cTnT staining (brown). Left panel: control. Right panel: CSA treatment. Scale bars = 400 μm. **B.** Quantitative evaluation of cardiomyocyte induction by fluorescent intensity of cTnT staining. Relative fluorescent intensity is

indicated (n = 4, †, $p<0.001$ vs control). **C.** Representative action potential of iPSC-derived spontaneously beating cardiomyocytes. **D.** Sarcomeric organization in TMRM-purified cardiomyocytes at Flk-d8. Immunostaining with anti-sarcomeric α-actinin antibody (red) and DAPI (blue). Right panel shows higher magnification of boxed area. Scale bar = 25 μm. **E–H.** Double immunostaining of TMRM-purified cardiomyocytes at Flk-d8 for connexin43 (Cx43) (green) and cTnT (orange) (E), Cav3.2 (green) and cTnT (orange) (F), HCN4 (green) and cTnT (orange) (G), Kir2.1 (green) and cTnT (orange) (H). Nuclei are visualized with DAPI. Scale bars = 25 μm. I. FACS analysis for cardiac progenitor induction from mouse iPSCs by CSA. X axis: CXCR4. Y axis: Flk1. Percentages of FCV cardiac progenitor cells (double positive population; red boxes) in total $Flk1^+$ cell progenies are indicated.
doi:10.1371/journal.pone.0016734.g001

Flowcytometry and cell sorting

FACS for differentiating mouse iPSCs was performed as described previously [8], [12], [20]. After 96–108 h of iPSC differentiation, cultured cells were harvested and stained with allophycocyanin (APC)-conjugated AVAS12 and FITC-conjugated ECCD2. Viable $Flk1^+$/E-cadherin$^-$ cells, excluding propidium iodide (Sigma), were sorted by FACS AriaII (Becton Dickinson). For FACS for FCV progenitor cells, after 2 days differentiation of purified $Flk1^+$ cell on PKH67-stained OP9 cells (Flk-d2), cultured cells were harvested and stained with a combination of MoAbs of PE-conjugated AVAS12 and biotinylated CXCR4 followed by addition of streptoavidin-conjugated APC, and subjected to FACS analysis. PKH-negative populations were analyzed and sorted as iPSC-derived cells. The $Flk1^+$/$CXCR4^+$ population (which was vascular endothelial cadherin-negative) [8] was designated "FCV cells". For FACS for cardiomyocytes, cells were harvested after 6–8 days culture of $Flk1^+$ cells on OP9 cells (Flk-d6-8). Induced cardiomyocytes were selected using tetramethyl rhodamine methyl ester (TMRM) (Invitrogen) [12], a fluorescent probe to monitor the membrane potential of mitochondria. In brief, cells were dissociated with 0.25% tryprin/EDTA, then incubated in DM with 50 nmol/L TMRM at 37°C for 15 minutes. Stained cells were washed twice and selected by FACS. TMRM-high population was considered as purified cardiomyocytes in iPSCs.

Human iPSC culture

END-2 cells were cultured as described previously [31]. Human iPS cell lines induced with transduction of four transcription factors (Oct4, Sox2, Klf4, and c-myc), 201B6 and 201B7, and Myc-negative human iPSC lines, 253G1 and 253G4 were maintained as previously described [1], [32]. 253G1 was used as the human iPS cell representative in all experiments unless stated otherwise. Induction of cardiomyocyte differentiation from human iPSCs was performed by co-culturing clumps of undifferentiated human iPSCs on END-2 cells, essentially as described previously [31]. To study the effect of CSA on cardiomyocyte differentiation, 3 μg/mL CSA was added to the culture medium on day 0 (END2-d0) or 8 (END2-d8) after start of co-culture. The number of beating colonies on END2-d12 was scored by microscopic examination. For intracellular Ca^{++} measurement and immunostaining for cTnT and actinin, beating colonies were mechanically excised, then gently dissociated by trypsin-EDTA treatment (at 37°C, 10 min), and replated on to gelatin-coated dishes. For electrophysiological analysis, beating colonies were mechanically excised and then dissociated by trypsin-EDTA with DNAse I (at 37°C, 10–15 min), and replated on to gelatin-coated dishes.

Immunohistochemistry

Immunostaining of murine cardiomyocytes was performed as described [8], [11], [12]. Briefly, 4% paraformaldehyde (PFA)-fixed cells were blocked by 2% skimmed milk (BD, bioscience) and incubated with 1st Abs. For immunohistochemistry, anti-mouse IgG –horse radish peroxidase (HRP) (Invitrogen) was used as 2nd Abs. For immunofluorescent staining, anti-mouse, rat and rabbit immunoglobulin conjugated with Alexa 488 or 546 were used for 2nd Abs. Nuclei were visualized with DAPI (Invitrogen). Cardiomyocyte differentiation was quantified as the fluorescent intensity of cTnT staining as described [8]. Immunostaining for human cardiomyocytes, 4% paraformaldehyde (PFA)-fixed cells were processed with 0.2% Triton X100 and 1% BSA (Sigma), and incubated with 1st Abs. Stained cells were photographed with inverted fluorescent microscopy, Eclipse TE2000-U (Nikon, Tokyo, Japan), digital camera system, AxioCam HRc (Carl Zeiss, Germany), or BIOREVO BZ-9000 (Keyence, Osaka, Japan).

Electrophysiology

Membrane potentials of single cells within a beating colony were measured using whole-cell patch clamp electrophysiology in the current-clamp mode (Axopatch200B, Axon Instruments/Molecular Devices Corp., Union City, CA). All recordings were carried out at room temperature [8].

Buffer compositions. Bath solution contained (in mmol/L) 140 NaCl, 5.4 KCl, 0.33 NaH_2PO_4, 0.45 $MgCl_2$, 1.8 $CaCl_2$, and 5 HEPES (pH = 7.4 with NaOH). Pipette solution contained (in mmol/L) 110 L-Aspartic acid, 30 KCl, 5 MgATP, 0.1 NaGTP, 5 K_2Creatine phosphate, 2 EGTA, 10 HEPES, and 10 NaOH (pH = 7.2 with KOH).

Field potential (FP) recordings of the beating colonies were performed using The MED64 multi-electrode array (MEA) system (Alpha MED Scientific Inc., Osaka, Japan) at a sampling rate of 20 kHz with low path filter of 500 Hz or high path filter of 1 Hz. All MEA measurements were performed at 37°C with heated perfusion system. The signals were recorded and processed with the Mobius software (WitXerx, US). The medium were perfused 1.7 ml/min as 37°C, and then the FPs were recorded for 5 min. Subsequently, E-4031(Calbiochem, US), isoproterenol (Proternol-L®, Kowa Pharmaceutical Company, Tokyo, Japan), or propranprol (Inderal®, AstraZeneca, Japan) was added to medium (discrete colony samples were used for each drug). Then, the FPs were measured for about 10 min.

Intracellular Ca measurement

Human iPSCs were loaded with 4 μM Quest Fluo-8 (ABD Bioquest, Inc. Sunnyvale, CA) for 30 min. Fluo-8 fluorescence (excitation at 495±10 nm and emission at 535±20 nm) of beating colony was measured every 16 msec with a back-thinned electron multiplier CCD camera (ImagEM; Hamamatsu Photonics, Hamamatsu, Japan). Four consecutive images were averaged. Ratio (F1/F0) to an image at minimum fluorescence intensity (F0) was calculated after background subtraction. The measurements were carried out at room temperature.

Reverse Transcription Polymerase Chain Reaction (RT-PCR)

Total RNA was isolated from various kinds of cell populations with the use of RNeasy Mini Kit (QIAGEN, Valencia, CA). cDNA was synthesized by the SuperScript III First-strand Synthesis System (Invitrogen). Polymerase chain reaction was performed with the use of KOD Plus (Toyobo, Tokyo, Japan) as described [33]. Primer sequences [34] are shown in Table S1.

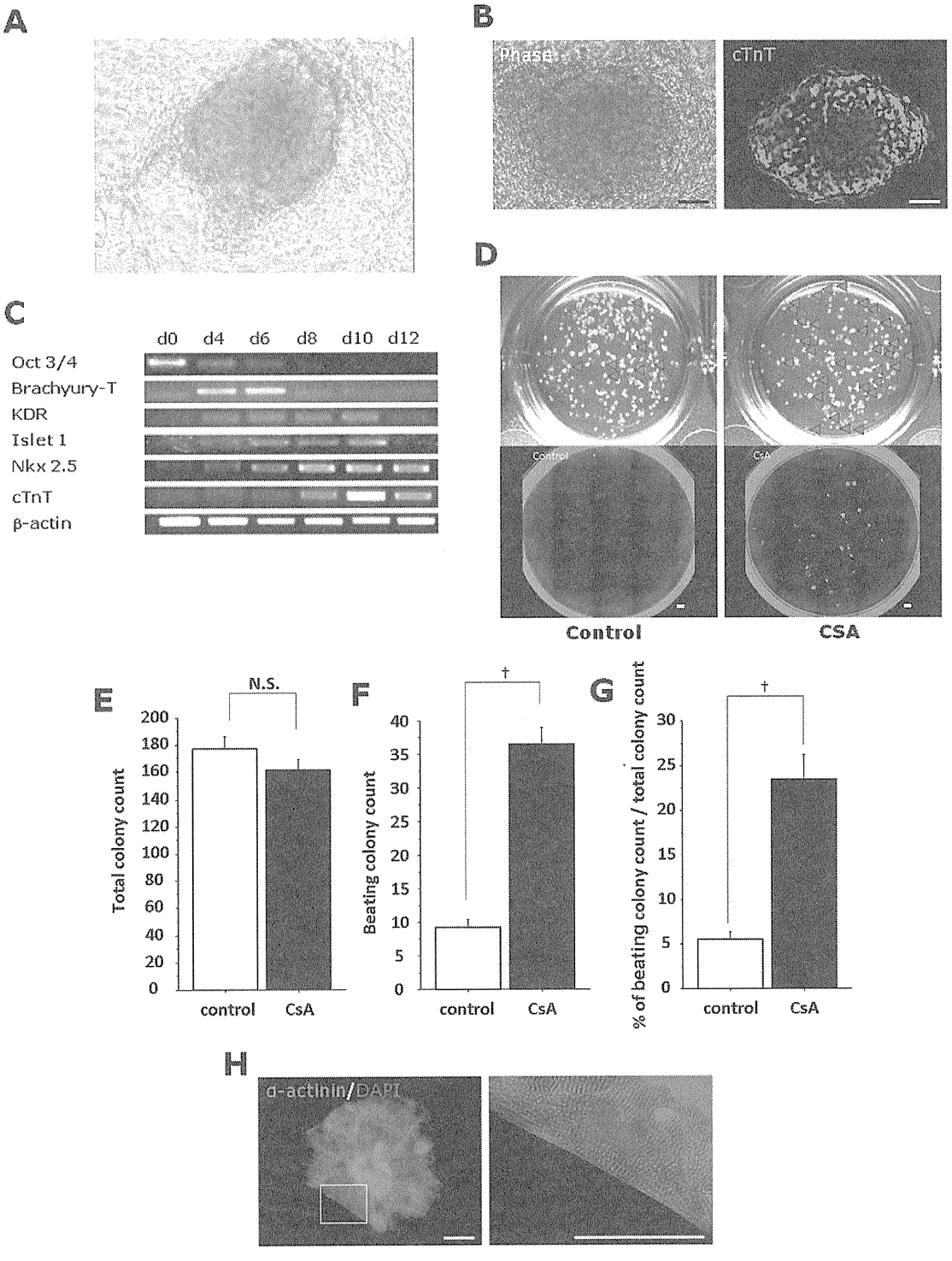

Figure 2. Induction and expansion of cardiomyocytes from human iPSCs. Human iPSCs were co-cultured with END-2 cells to differentiate cardiomyocytes. **A.** Gross morphology of a beating colony from human iPSCs (captured photo from Movie S1). **B.** cTnT staining of a beating colony on END-2 cells. Left panel: phase contrast image. Right panel: human cTnT staining (green). Scale bar = 50 μm. **C.** RT-PCR analysis for differentiation markers during cardiomyocyte differentiation of human iPSCs (from END2-d0 to d12). Oct3/4: Undifferentiated cell marker, Brachyury-T: mesendoderm marker, KDR (human Flk1): mesoderm marker, Islet1: mesoderm and cardiac progenitor marker, Nkx2.5: cardiac progenitor and cardiomyocyte marker, cTnT: cardiomyocyte marker. **D.** Representative gross appearance of human iPSC-derived beating colonies at END2-d12 in 12-well dishes. Left panels: control. Right panels: CSA treatment from END2-d8. Upper panels: phase contrast images. Beating colonies are shown by red arrows. Lower panels: cTnT staining (green). **E–G** Quantitative evaluation of beating colony appearance. **E.** Total colony count (control; 177±9.7/well (12-well dishes)(n = 8), CSA; 162±8.0/well (n = 9); N.S., p = 0.237), **F.** Beating colony count (control; 9.1±1.2/well (12-well dishes)(n = 8), CSA; 36.4±2.5/well (n = 9); †, p<0.0001), and **G.** Percentages of beating colonies (control; 5.4±0.9% (n = 8), CSA; 23.5±2.8% (n = 9); †, p<0.0001) in total colonies that appeared at END2-d12. **H.** Immunostaining of actinin (red) and DAPI (blue) in dissociated cardiomyocyte colonies. The same colony is shown in Movie S2. Right panel shows higher magnification of boxed area. Sarcomere structures are evident. Scale bar = 50 μm.
doi:10.1371/journal.pone.0016734.g002

Electron microscopic study

Human iPSC-derived beating colony was replated on multi-well chamber slide (NUNC Rochester, NewYork), fixed with 2% glutaraldehyde in 0.1 mol/L phosphate buffer (pH 7.4) for 30–60 min, washed and immersed with phosphate buffered saline for overnight at 4°C, and fixed in 1% buffered osmium tetroxide. The specimens were then dehydrated through graded ethanol and embedded in epoxy resin. Ultrathin sections (90 nm), double-stained with uranyl acetate and lead citrate, were examined under electron microscopy (H-7650; Hitachi, Tokyo, Japan).

Statistical Analysis

All data were obtained from at least three independent experiments. Statistical analysis of the data was performed using Student's t-test or ANOVA. $p<0.05$ was considered significant. All data are shown as mean ± S.D.

Results

Cardiomyocyte and cardiac progenitor expansion from mouse iPSCs by CSA

Recently, we reported that functional cardiomyocytes were induced from mouse iPSCs with our differentiation method in mouse ES cells [12]. In brief, undifferentiated mouse iPSC colonies maintained on MEFs were morphologically similar to mouse ESCs. We induced mesoderm differentiation from mouse iPSCs by culturing on type IV collagen-coated dish with DM (see Methods). $Flk1^+$ mesoderm cells that appeared were selected by FACS at 4.5 days of differentiation (iPS-d4.5) and then underwent a cardiomyocyte induction protocol involving co-culture on OP9 stroma cells; spontaneously beating cardiomyocytes began to appear after 3 to 4 days of culture (Flk-d3-4). Beating cells that appeared were positive for multiple cardiomyocyte markers and had electrophysiological features assessed by whole-cell patch clamp as previously reported [8], [12].

In the present study, we first tried to expand cardiomyocytes and cardiac progenitors from mouse iPS cells by CSA. When CSA was added to purified $Flk1^+$ cells, the appearance of $cTnT^+$ cardiomyocytes was increased 12-fold compared to controls (Fig. 1A, B), which was comparable with the increase observed in mouse ESCs [11]. CSA-expanded cardiomyocytes spontaneously beat and showed cardiomyocyte-like action potential (average interval: 0.74 sec, maximum diastolic potential: −58.6 mV and overshoot: 34.3 mV (n = 6)) (Fig. 1C). These cardiomyocytes also showed distinct sarcomere formation (Fig. 1D), expression of cTnT (Fig. 1E-H) and connexin 43 located at cellular boundaries (Fig. 1E). T-type calcium channel Cav3.2 (Fig. 1F), a pacemaker ion channel, HCN4 (Fig. 1G), and a ventricular ion channel, kir2.1 (Fig. 1H) were also detected in $cTnT^+$ cells. We also examined the effect of CSA on the induction of FCV cardiac progenitor cells in mouse iPSCs. Addition of CSA to $Flk1^+$ cells specifically increased the FCV population in mouse iPSCs to approximately 6.5 times of control. The maximum percentage of FCV cells within total $Flk1^+$ cell-derived cells was more than 30% by CSA (Fig. 1I), comparable with that observed in mouse ESCs, previously [11]. CSA can thus efficiently enhance the differentiation of functional cardiomyocytes and cardiac progenitors from mouse iPSCs.

Differentiation of cardiomyocytes from human iPSCs

We next examined cardiomyocyte differentiation from human iPSCs. We employed a human ESC differentiation method for cardiomyocytes using END-2 visceral endodermal stroma cells [31]. When human iPSCs were cultured on END-2 cells, spontaneously beating cardiomyocytes were successfully induced (Fig. 2A, Movie S1). Beating colonies were first detected after END2-d10 and became maximally evident after END2-d12.

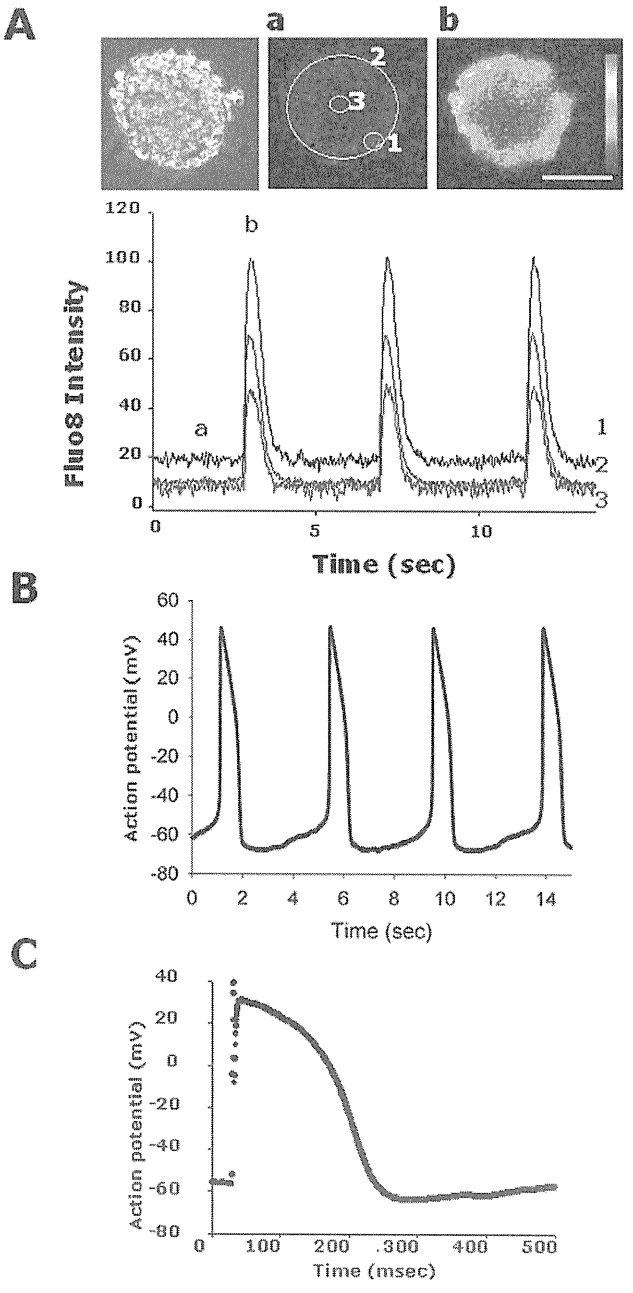

Figure 3. Functional analysis of expanded human cardiomyocytes. A. Ca^{++} transient in dissociated beating colonies. Cytoplasmic Ca^{++} change was monitored with fluo-8. Left panel: a transmission image of fluo-8 loaded iPSC colony. Middle and right panels: Fluo-8 images at the end (a) and the peak (b) of the fluorescence change. Scale bar = 50 μm. Lower panel: Time course of fluo-8 intensity change. The intensity was measured at the periphery (1), the entire colony (2) and the center (3) (ROIs shown in middle panel). Ratios (F1/F0) of the intensity to the one at the beginning of recording (F0) are indicated. Note that Ca transient is well synchronized within the colony. Real time video is shown in Movie S3. **B.** Representative action potential recorded from a cell in a beating colony. **C.** Representative single whole cell patch-cramp recording of a non-self beating human iPSC-derived cardiomyocyte after electrical stimulation.
doi:10.1371/journal.pone.0016734.g003

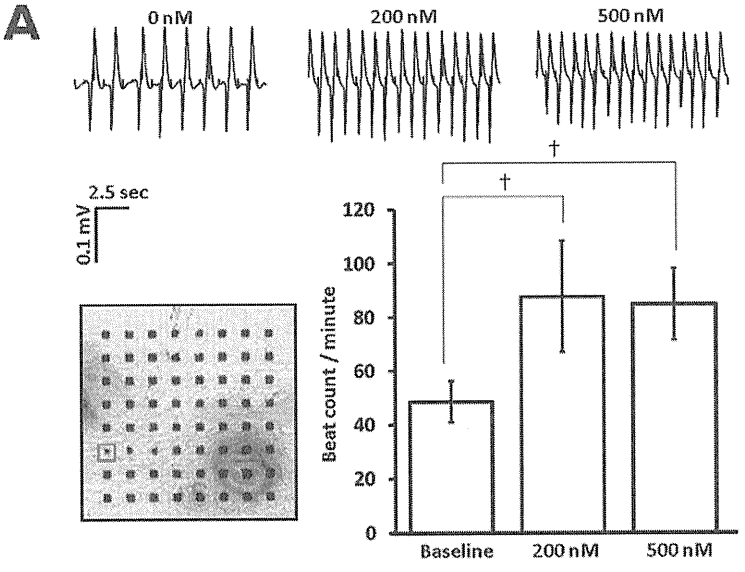
A
0 nM
200 nM
500 nM
2.5 sec
0.1 mV
Beat count / minute
120
100
80
60
40
20
0
Baseline
200 nM
500 nM
†
†

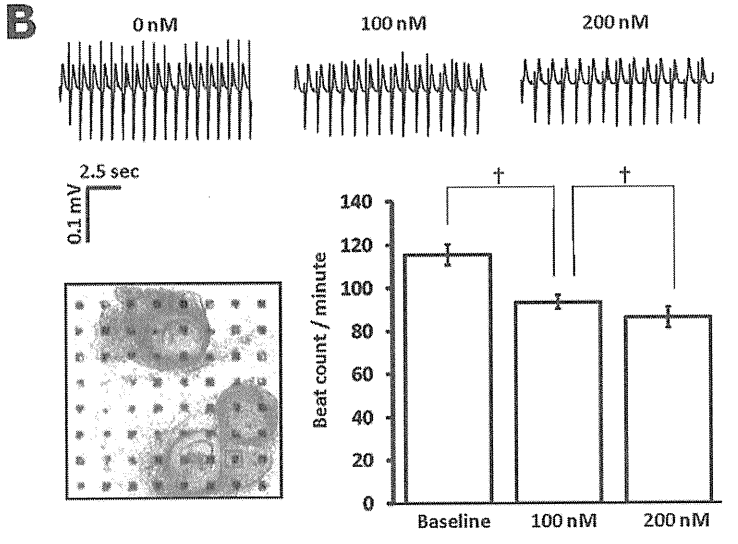
B
0 nM
100 nM
200 nM
2.5 sec
0.1 mV
Beat count / minute
140
120
100
80
60
40
20
0
Baseline
100 nM
200 nM
†
†

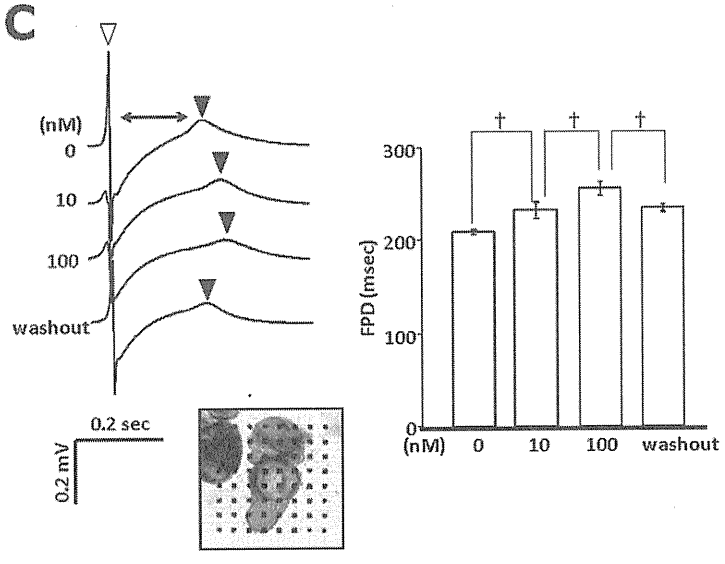
C
(nM)
0
10
100
washout
0.2 sec
0.2 mV
FPD (msec)
300
200
100
0
(nM) 0 10 100 washout
†
†
†

Figure 4. Pharmacological responses of human iPSC-derived cardiomyocytes. Field potential recordings of replated beating colonies after stimulation with isoproterenol (**A**), propranorol (**B**), and E-4031 (**C**). Photos; array of multi-electrode and replated colonies. Data recorded at electrodes in red squares are shown. **A, B.** Beating frequency (beating/minite). **C.** QT elongation. The time period from the first negative peak (open triangle) to the first positive peaks (closed triangles) reflects QT time in electrocardiogram. n = 3, †, $p<0.001$.
doi:10.1371/journal.pone.0016734.g004

These beating colonies were positive for cTnT (Fig. 2B). During the differentiation of human iPSCs on END2 cells, sequential expression of various marker genes expected for cardiomyogenesis was observed (ex: Oct3/4; undifferentiated iPSCs, Brachyury; mesendoderm, KDR; mesoderm, islet1; mesoderm and cardiac progenitors, nkx2.5; cardiac progenitors and cardiomyocytes, cTnT; cardiomyocytes) (Fig. 2C). In our another previous study on human ESC differentiation, a Flk1 (in human, VEGF receptor-2)$^{+}$/TRA1-60^{-} mesoderm population appeared in culture approximately 8 days after induction of differentiation [35]. When CSA was added to differentiating human iPSCs at the mesoderm stage (i.e. on END2-d8), the appearance of beating colonies was increased (Fig. 2D) although no effect was observed with the CSA treatment on undifferentiated human iPSCs (i.e. from END2-d0) (data not shown). Whereas the total number of iPSC-derived colonies that appeared was not changed (Fig. 2E), the number and percentage of beating colonies that appeared at END2-d12 were significantly increased approximately 4.0 and 4.3 times by CSA treatment, respectively (Fig. 2F, G). Approximately 23±2.7% of total colonies was beating in average, and in an optimized condition, 39% of total colonies included beating cardiomyocytes. CSA-expanded colonies maintained self-beating after a mechanical isolation and re-plating, and were positive for α-actinin with distinct sarcomere formation (Fig. 2H, Movie S2). Thus, cardiomyocyte induction from human iPSCs could be similarly enhanced by CSA. The mesoderm stage-specific effect of CSA in human iPSCs suggests the similar machinery in mouse ES/iPSCs are robustly working in human iPSC differentiation to cardiomyocytes.

Functional features of expanded human iPSC-derived cardiomyocytes

We next evaluated functional features of CSA-expanded human iPSC-derived cardiomyocytes. Fluo-8 imaging revealed synchronized increases in intracellular Ca^{++} in beating colonies with contraction (Fig. 3A, Movie S3). Action potentials recorded by patch clamp electrophysiology identified cells with pacemaker potential (average of the interval: 4.26 sec, maximum diastolic potential: −67.6 mV overshoot: 46.6 mV (n = 6))(Fig. 3B). Replated colonies continued beating spontaneously for more than 10 months. Some isolated single cells obtained from beating colonies at 3 months culture period lost automaticity and showed some features of human ventricular cells such as action potential with rapid depolarization and prolonged plateau after electrical stimulation (Fig. 3C). These results indicate that various functional human cardiomyocytes could be induced in this system.

We further examined pharmacological reactions of CSA-expanded human cardiomyocytes to show the relevance as cardiac cell models. We recorded field potential of re-plated beating colonies with multi-electrode array under simulation of a β-stimulant, isoproterenol, a β-blocker, propranorol, and a HERG channel inhibitor, E-4031. Addition of isoproterenol significantly increased the beating frequency (Fig. 4A), on the other hand, propranorol significantly decreased the beating frequency (Fig. 4B). E-4031 dose-dependently prolonged the length of time from the first negative peak to first positive peak, which is corresponding to QT time in electrocardiogram (Fig. 4C). These results indicate that CSA-expanded human iPSC-derived cardiomyocytes can suffice multiple functional features as human cardiomyocyte cell models.

Ultra structural features of expanded human iPSC-derived cardiomyocytes

We finally confirmed features of CSA-expanded human iPSC-derived cardiomyocytes at the ultrastructural level using electron microscopy. Beating colonies induced from human iPSCs resembled native cardiomyocytes, showing myofibrillar bundles with transverse Z-bands and enriched mitochondria (Fig. 5A-D). Other cardiomyocyte-specific structures, such as intercalated disks with desmosomes (Fig. 5D), atrial secretory granule-like structures (Fig. 5E), and glycogen granules (Fig. 5F) were also observed.

Together, these results indicate that *bona fide* human cardiomyocytes can be successfully induced and expanded from human iPSCs with this method.

Discussion

Here we demonstrated the induction and expansion of cardiac progenitors and functional cardiomyocytes from iPSCs using potent and specific effect of CSA. Human cardiomyocytes with multiple expected structural and functional features could be induced with this method. This method provides a critical technological basis to obtain cardiac cells from human iPSCs.

We have demonstrated previously that CSA treatment is most effective in inducing FCV cardiac progenitor cells, the nearest upstream of cardiomyocytes in mouse ESCs [11]. Here we showed that CSA effects on FCV cardiac progenitor and cardiomyocyte induction were also completely reproduced in mouse iPSCs. Moreover, CSA also showed significant enhancing effects of cardiomyocyte differentiation from human iPSCs in the END-2 system. This is the first report to show the effect of CSA in human stem cells. In this study, we examined four human iPSC clones, 201B6, B7 (induced with four factors) [1], 253G1 and G4 (induced without c-myc) [32]. Though the basal efficiency of cardiomyocyte differentiation from 201B6, B7 and 253G4 were lower than that from 253G1, CSA treatment significantly enhanced cardiomyocyte appearance similarly in all these human iPSC clones (Figure S1). Thus, CSA robustly induced cardiogenic differentiation in mouse ESCs, iPSCs and human iPSCs regardless their species and derivation methods.

The molecular mechanisms conducting this potent CSA effect on cardiac lineage is important, but still it is unknown. Though we examined another calcineurin inhibitor, FK506, and a NF-AT inhibitor, 11R-VIVIT, both of them did not reproduce the effect of CSA [11], indicating that the cardiogenic CSA effect is mediated by other molecular target than immunosuppressing effect of CSA. Further elucidation of molecular mechanisms of CSA in cardiomyocyte differentiation would be critical for the exploration of cardiomyocyte differentiation and regeneration strategies.

CSA-expanded cardiomyocytes from human iPSCs exhibited many features sufficing as functional cardiomyocytes. Cardiomyocytes with pacemaker-like or ventricular-like action potentials were successfully induced. Nevertheless, they were still immature compared with mature adult cardiomyocytes [36], [37] and they

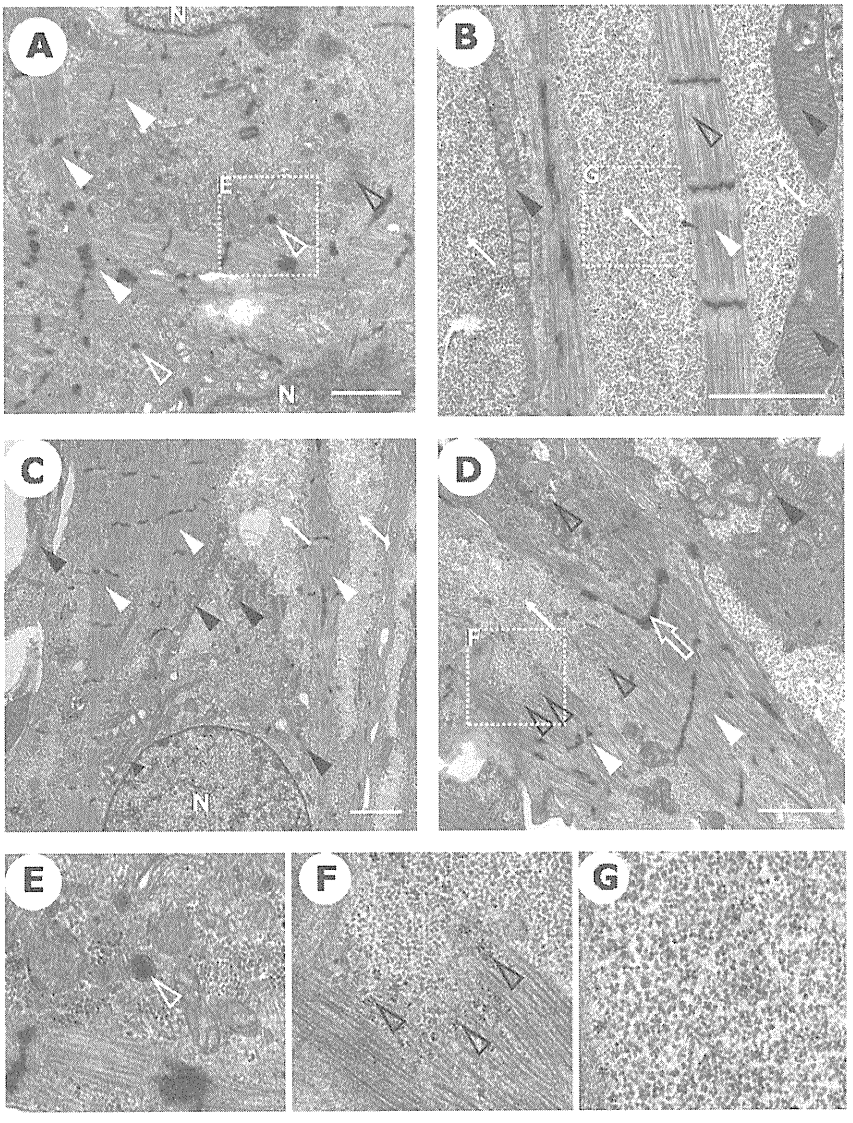

Figure 5. Ultrastructural analysis of human iPSC-derived cardiomyocytes. Transmission electron microscopic images of beating colonies. Myofibrils with Z-bands (white closed arrowheads in **A–D.**), mitochondria (black closed arrowheads in **B–D.**), intercalated disk-like structure with desmosome (white open arrow in **D.**), atrial sercetory granules (electron-dense granules surrounded by double membranes. White open arrowheads in **A.** and **E.** (magnified image of **A.**)), glycogen granules (electron-dense small granules. Black open arrowheads in **D.** and **F.** (magnified image of **D.**)), ribosomal granules (electron-lucent small granules. White arrows in **B–D.** and **G.** (magnified image of **B.**)). N: nucleus. Scale bar = 2 μm, direct magnify, ×3000 (A), ×7000 (B), ×4000 (C), ×5000 (D).
doi:10.1371/journal.pone.0016734.g005

also displayed some structural features of fetal cardiomyocytes, such as relatively low global electron density, sparse myofibrils, and abundant ribosome granules (Fig. 5). Methods for further maturation as well as specific induction and purification of the various cardiac cell types (pacemaker, atrial, ventricular, conduction system cells etc.) should be explored in future study.

Interestingly, a recent clinical report showed that CSA prevented cardiac reperfusion injury by protecting cardiomyocytes from apoptosis [38]. Cardiogenic effects of CSA in later stages of differentiation of human iPSCs imply that CSA may positively affect on endogenous cardiac progenitors to induce cardiac regeneration in patients. Though it is still unknown whether endogenous cardiac regeneration can be induced by CSA administration, our study may offer a scientific basis to support a clinical opportunity for CSA as a cardiac regenerative drug.

This novel cardiac cell differentiation method for iPSCs would thus broadly contribute to cardiac regenerative medicine by providing various options for cell preparation, transplantation strategies, and drug discovery.

Supporting Information

Figure S1 Quantitative evaluation of beating colony appearance in iPSC clones. 201B6 cells: Total colony count (control; 203±6.4/well (12-well dishes)(n = 3), CSA; 193±4.0/well (n = 3); N.S., p = 0.0915), beating colony count (control; 4.0±1.0/well (n = 3), CSA; 13.7±3.5/well (n = 3); *, $p<0.05$), percentages of beating colonies (control; 2.0±0.5% (n = 3), CSA; 7.1±1.7% (n = 3); **, $p<0.01$) in total colonies that appeared at END2-d12. 201B7 cells: Total colony count (control; 204±8.3/well (n = 3),

CSA; 200±2.0/well (n = 3); N.S., p = 0.43), beating colony count (control; 5.0±1.0/well (n = 3), CSA; 18.3±3.1/well (n = 3); **, p<0.01), percentages of beating colonies (control; 2.5±0.6% (n = 3), CSA; 9.2±1.5% (n = 3); **, p<0.01). 253G4 cells: Total colony count (control; 201±4.0/well (n = 3), CSA; 201±3.8/well (n = 3); N.S., p = 0.9216), beating colony count (control; 4.7±0.6/well (n = 3), CSA; 15.0±1.0/well (n = 3); **, p<0.05), percentages of beating colonies (control; 2.3±0.3% (n = 3), CSA; 7.5±0.6% (n = 3); †, p<0.001)
(TIF)

Movie S1 A beating colony induced from human iPS cells at END2-d12 (Fig. 2A).
(MOV)

Movie S2 A dissociated beating colony induced from human iPS cells on END-2 cells (Fig. 2H).
(MOV)

Movie S3 Real time monitoring of Ca^{++} transient by Fluo-8 in dissociated beating colony induced from human iPS cells (Fig. 3A). Clear and synchronized Ca^{++} transient is observed.
(MOV)

Table S1 Primers for PCR.
(RTF)

Acknowledgments

We thank Dr. D. Ward (Leiden University Medical Center) for supplying END-2 cells, Dr. G. Takemura (Gifu University Graduate School of Medicine) for interpretation and evaluation of electron microgram, Novartis Pharma for providing cyclosporin-A, Dr. M. Takahashi (Kyoto University Graduate School of Medicine) for critical reading of the manuscript.

Author Contributions

Conceived and designed the experiments: MF PY JKY. Performed the experiments: MF PY TGO GN HU HF HM SM. Analyzed the data: MF TI CLM JKY. Contributed reagents/materials/analysis tools: KO KT MN CLM. Wrote the paper: MF RS CLM NN KN SY JKY.

References

1. Takahashi K, Tanabe K, Ohnuki M, Narita M, Ichisaka T, et al. (2007) Induction of pluripotent stem cells from adult human fibroblasts by defined factors. Cell 131: 861–872.
2. Takahashi K, Yamanaka S (2006) Induction of pluripotent stem cells from mouse embryonic and adult fibroblast cultures by defined factors. Cell 126: 663–676.
3. Yamanaka S (2007) Strategies and new developments in the generation of patient-specific pluripotent stem cells. Cell Stem Cell 1: 39–49.
4. Nishikawa S, Goldstein RA, Nierras CR (2008) The promise of human induced pluripotent stem cells for research and therapy. Nat Rev Mol Cell Biol 9: 725–729.
5. Reinecke H, Minami E, Zhu WZ, Laflamme MA (2008) Cardiogenic differentiation and transdifferentiation of progenitor cells. Circ Res 103: 1058–1071.
6. Laflamme MA, Murry CE (2005) Regenerating the heart. Nat Biotechnol 23: 845–856.
7. Passier R, Oostwaard DW, Snapper J, Kloots J, Hassink RJ, et al. (2005) Increased cardiomyocyte differentiation from human embryonic stem cells in serum-free cultures. Stem Cells 23: 772–780.
8. Yamashita JK, Takano M, Hiraoka-Kanie M, Shimazu C, Peishi Y, et al. (2005) Prospective identification of cardiac progenitors by a novel single cell-based cardiomyocyte induction. FASEB J 19: 1534–1536.
9. Kattman SJ, Huber TL, Keller GM (2006) Multipotent Flk-1^+ cardiovascular progenitor cells give rise to the cardiomyocyte, endothelial, and vascular smooth muscle lineages. Dev Cell 11: 723–732.
10. Fukuda K, Yuasa S (2006) Stem cells as a source of regenerative cardiomyocytes. Circ Res 98: 1002–1013.
11. Yan P, Nagasawa A, Uosaki H, Sugimoto A, Yamamizu K, et al. (2009) Cyclosporin-A potently induces highly cardiogenic progenitors from embryonic stem cells. Biochem Biophys Res Commun 379: 115–120.
12. Narazaki G, Uosaki H, Teranishi M, Okita K, Kim B, et al. (2008) Directed and systematic differentiation of cardiovascular cells from mouse induced pluripotent stem cells. Circulation 118: 498–506.
13. Mauritz C, Schwanke K, Reppel M, Neef S, Katsirntaki K, et al. (2008) Generation of functional murine cardiac myocytes from induced pluripotent stem cells. Circulation 118: 507–517.
14. Schenke-Layland K, Rhodes KE, Angelis E, Butylkova Y, Heydarkhan-Hagvall S, et al. (2008) Reprogrammed mouse fibroblasts differentiate into cells of the cardiovascular and hematopoietic lineages. Stem Cells 26: 1537–1546.
15. Zhang J, Wilson GF, Soerens AG, Koonce CH, Yu J, et al. (2009) Functional cardiomyocytes derived from human induced pluripotent stem cells. Circ Res 104: e30–41.
16. Tanaka T, Tohyama S, Murata M, Nomura F, Kaneko T, et al. (2009) In vitro pharmacologic testing using human induced pluripotent stem cell-derived cardiomyocytes. Biochem Biophys Res Commun 385: 497–502.
17. Yokoo N, Baba S, Kaichi S, Niwa A, Mima T, et al. (2009) The effects of cardioactive drugs on cardiomyocytes derived from human induced pluripotent stem cells. Biochem Biophys Res Commun 387: 482–488.
18. Zwi L, Caspi O, Arbel G, Huber I, Gepstein A, et al. (2009) Cardiomyocyte differentiation of human induced pluripotent stem cells. Circulation 120: 1513–1523.
19. Moretti A, Bellin M, Jung CB, Thies TM, Takashima Y, et al. (2010) Mouse and human induced pluripotent stem cells as a source for multipotent $Isl1^+$ cardiovascular progenitors. FASEB J 24: 700–711.
20. Yamashita J, Itoh H, Hirashima M, Ogawa M, Nishikawa S, et al. (2000) Flk1-positive cells derived from embryonic stem cells serve as vascular progenitors. Nature 408: 92–96.
21. Nishikawa SI, Nishikawa S, Hirashima M, Matsuyoshi N, Kodama H (1998) Progressive lineage analysis by cell sorting and culture identifies $FLK1^+VE$-$cadherin^+$ cells at a diverging point of endothelial and hemopoietic lineages. Development 125: 1747–1757.
22. Kataoka H, Takakura N, Nishikawa S, Tsuchida K, Kodama H, et al. (1997) Expressions of PDGF receptor alpha, c-Kit and Flk1 genes clustering in mouse chromosome 5 define distinct subsets of nascent mesodermal cells. Dev Growth Differ 39: 729–740.
23. Yamashita J (2004) Cardiovascular cell differentiation from ES cells. In: Mori H, Matsuda H, eds. Cardiovascular Regeneration Therapies Using Tissue Engineering Approaches. Tokyo: Springer-Verlag GmbH, Chapter 2. pp 67–80.
24. Moretti A, Caron L, Nakano A, Lam JT, Bernshausen A, et al. (2006) Multipotent embryonic $isl1^+$ progenitor cells lead to cardiac, smooth muscle, and endothelial cell diversification. Cell 127: 1151–1165.
25. Wu SM, Fujiwara Y, Cibulsky SM, Clapham DE, Lien CL, et al. (2006) Developmental origin of a bipotential myocardial and smooth muscle cell precursor in the mammalian heart. Cell 127: 1137–1150.
26. Garry DJ, Olson EN (2006) A common progenitor at the heart of development. Cell 127: 1101–1104.
27. Yamashita JK (2007) Differentiation of arterial, venous, and lymphatic endothelial cells from vascular progenitors. Trends Cardiovasc Med 17: 59–63.
28. Yamashita JK (2004) Differentiation and diversification of vascular cells from embryonic stem cells. Int J Hematol 80: 1–6.
29. Yanagi K, Takano M, Narazaki G, Uosaki H, Hoshino T, et al. (2007) Hyperpolarization-activated cyclic nucleotide-gated channels and T-type calcium channels confer automaticity of embryonic stem cell-derived cardiomyocytes. Stem Cells 25: 2712–2719.
30. Okita K, Ichisaka T, Yamanaka S (2007) Generation of germline-competent induced pluripotent stem cells. Nature 448: 313–317.
31. Mummery C, Ward-van Oostwaard D, Doevendans P, Spijker R, van den Brink S, et al. (2003) Differentiation of human embryonic stem cells to cardiomyocytes: role of coculture with visceral endoderm-like cells. Circulation 107: 2733–2740.
32. Nakagawa M, Koyanagi M, Tanabe K, Takahashi K, Ichisaka T, et al. (2008) Generation of induced pluripotent stem cells without Myc from mouse and human fibroblasts. Nat Biotechnol 26: 101–106.
33. Yamamizu K, Kawasaki K, Katayama S, Watabe T, Yamashita JK (2009) Enhancement of vascular progenitor potential by protein kinase A through dual induction of Flk-1 and Neuropilin-1. Blood 114: 3707–3716.
34. Yang L, Soonpaa MH, Adler ED, Roepke TK, Kattman SJ, et al. (2008) Human cardiovascular progenitor cells develop from a KDR^+ embryonic-stem-cell-derived population. Nature 453: 524–528.
35. Sone M, Itoh H, Yamahara K, Yamashita JK, Yurugi-Kobayashi T, et al. (2007) Pathway for differentiation of human embryonic stem cells to vascular cell components and their potential for vascular regeneration. Arterioscler Thromb Vasc Biol 27: 2127–2134.
36. Chacko KJ (1976) Observations on the ultrastructure of developing myocardium of rat embryos. J Morphol 150: 681–709.
37. Kehat I, Kenyagin-Karsenti D, Snir M, Segev H, Amit M, et al. (2001) Human embryonic stem cells can differentiate into myocytes with structural and functional properties of cardiomyocytes. J Clin Invest 108: 407–414.
38. Piot C, Croisille P, Staat P, Thibault H, Rioufol G, et al. (2008) Effect of cyclosporine on reperfusion injury in acute myocardial infarction. N Engl J Med 359: 473–481.

Respiratory Medicine (2011) 105, 939–945

available at www.sciencedirect.com

ScienceDirect

journal homepage: www.elsevier.com/locate/rmed

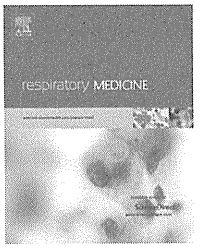

Comparison of biomarkers of subclinical lung injury in obstructive sleep apnea

Kensaku Aihara [a], Toru Oga [b,*], Yuka Harada [a], Yuichi Chihara [a], Tomohiro Handa [a], Kiminobu Tanizawa [a], Kizuku Watanabe [a], Tomomasa Tsuboi [b], Takefumi Hitomi [b], Michiaki Mishima [a], Kazuo Chin [b]

[a] *Department of Respiratory Medicine, Graduate School of Medicine, Kyoto University, Kyoto, Japan*
[b] *Department of Respiratory Care and Sleep Control Medicine, Graduate School of Medicine, Kyoto University, 54 Kawahara, Shogoin, Sakyo-ku, Kyoto 606-8507, Japan*

Received 17 December 2010; accepted 20 February 2011
Available online 12 March 2011

KEYWORDS
Obstructive sleep apnea;
KL-6;
Surfactant protein-D;
C-reactive protein;
Lung injury

Summary
Background: Obstructive sleep apnea (OSA) has both systemic and local effects partly through the increased oxidative stress caused by intermittent hypoxia and reoxygenation. However, lung-specific biomarkers in OSA have not been fully assessed in comparison with systemic biomarkers such as C-reactive protein (CRP), although results of a recent study having a small sample size indicated KL-6 as one candidate.
Methods: Subjects of the present study were 197 patients suspected to have OSA. In addition to polysomnography, we also measured serum levels of KL-6, surfactant protein-D (SP-D) and CRP and pulmonary function. We examined the relationships of different biomarkers with OSA severity and pulmonary function.
Results: The apnea/hypopnea index (AHI) was significantly positively correlated with serum KL-6 levels even after adjustment for body mass index (BMI) and smoking ($p = 0.03$), but not with SP-D and CRP. Also, a significant trend for an increase in serum KL-6 was noted in accordance with the severity of OSA even after adjustment for BMI and smoking (β coefficient $= 0.18$, $p = 0.02$). Additionally, elevated KL-6 levels were significantly associated with restrictive lung function disturbance and gas exchange derangement after adjustment for obesity and smoking, which contrasted with CRP whose elevations were significantly associated with worsened airflow limitation and increased lung volume.
Conclusions: Serum KL-6 levels may reflect the degree of subclinical lung injury associated with OSA independently of obesity or smoking, unlike CRP. We consider that KL-6 can be a potential candidate as a lung-specific biomarker of OSA and might provide complementary information on systemic biomarkers in assessing OSA.

* Corresponding author. Tel.: +81 75 751 3852; fax: +81 75 751 3854.
E-mail address: ogato@kuhp.kyoto-u.ac.jp (T. Oga).

0954-6111/$ - see front matter © 2011 Elsevier Ltd. All rights reserved.
doi:10.1016/j.rmed.2011.02.016

Introduction

Obstructive sleep apnea (OSA) is characterized by repeated episodes of upper airway obstruction accompanied by intermittent hypoxia and reoxygenation, which can cause oxidative stress.[1] It contributes not only to endothelial dysfunction in the peripheral circulation, but possibly also contributes to epithelial and endothelial cell injury in the alveolus causing increased alveolar wall permeability in the lungs.[2,3]

KL-6 is a mucin-like glycoprotein with a molecular weight of 200 kd and is mainly expressed on alveolar type II and bronchiolar epithelial cells in human lungs.[4] Elevated levels of circulating KL-6 have been reported in patients with lung injury.[5,6] Recently, Lederer et al. reported that circulating levels of KL-6 were elevated in some patients with OSA in association with greater endothelial dysfunction, suggesting that subclinical lung injury may be present in OSA.[7] However, the sample size in that study was very small, comprising only 11 OSA patients and 10 controls, and the relationships of elevated levels of KL-6 with other biomarkers or pulmonary function were not examined. Therefore, the role of KL-6 as a biomarker of lung injury in OSA has not been fully elucidated.

In addition to KL-6, circulating levels of surfactant protein-D (SP-D) are elevated in patients with lung injury.[8,9] SP-D is also exclusively produced by alveolar type II cells in the lungs and its values change with the clinical status of patients or with relevant exposures.[10] Therefore, recently, much attention has been paid to SP-D as a potential lung-specific biomarker in diseases such as chronic obstructive pulmonary disease (COPD) where both local and systemic inflammation play respective important roles in disease progression.[10,11] In OSA, increased levels of various systemic inflammatory biomarkers, including C-reactive protein (CRP), tumor necrosis factor-α, interleukin-6, and interleukin-8, have been reported to be associated with future cardiovascular risk.[12] Considering that OSA has respiratory and systemic effects, a lung-specific blood biomarker would be attractive and informative.

We hypothesized that higher serum levels of KL-6 and SP-D would be associated with more severe OSA and more severe impairments in pulmonary function, reflecting the degree of subclinical lung injury unlike CRP, which is the most widely studied systemic biomarker in OSA.[12] Although the magnitude of the injury might not be great, it may not only cause respiratory symptoms such as chronic cough[13] but also may worsen other possible comorbid disorders such as asthma,[14] COPD[15] or idiopathic pulmonary fibrosis (IPF).[16] Therefore, in the present study, we examined the relationships between these three different biomarkers, OSA and pulmonary function and assessed their clinical relevance.

Methods

Study subjects

A total of 197 patients were consecutively recruited from the Sleep Unit of Kyoto University Hospital between April 2009 and April 2010. All had been referred to our sleep unit with symptoms such as habitual snoring or daytime sleepiness. None had been previously diagnosed with or treated for OSA. Patients with pulmonary diseases such as asthma (n = 14), COPD (n = 5) or interstitial lung diseases (n = 2) and who were diagnosed as having central sleep apnea (n = 6) were excluded based on clinical history, spirometry, chest radiograph and polysomnography, and a total of 170 patients were examined further. This study was approved by the Kyoto University Graduate School and Faculty of Medicine Ethics Committee, and informed consent was obtained from all patients. Arterial blood gas analysis, including arterial partial tension of oxygen (PaO_2) and arterial partial tension of carbon dioxide ($PaCO_2$), was performed while patients were breathing room air at rest in the supine position. The alveolar-arterial oxygen tension difference ($A\text{-}aDO_2$) was calculated according to the standard formula, using the respiratory exchange ratio of 0.8.

Polysomnography

The diagnosis of OSA was confirmed by polysomnography (SomnoStar pro, Cardinal Health, Dublin, OH, USA), which was started at 22:00 and ended at 6:00 the following morning. Surface electrodes were attached using standard techniques to obtain an electrooculogram, electromyogram of the chin, and 12-lead electroencephalograph. Sleep stages were defined according to the criteria of Rechtschaffen and Kales.[17] Ventilation was monitored by inductive plethysmography (Respitrace QDC, Viasys Healthcare, Palm Springs, CA, USA). Airflow was monitored by a nasal pressure transducer (PTAFlite, Pro-Tech Services Inc., Mukilteo, WA, USA) and supplemented by an oronasal thermal sensor (Sleepmate Technologies, Midlothian, VA, USA). Arterial oxygen saturation (SpO_2) was monitored continuously with a pulse oximeter (Adult Flex System, Nonin Medical, Plymouth, MN, USA).

Apnea was defined as the complete cessation of airflow and hypopnea as a clear decrease in airflow of 50% or more lasting for 10 s or more accompanied by a decrease in SpO_2 of at least 3%.[18] All AHI values were expressed as the number of episodes of apnea and hypopnea per hour over the total sleep time. The lowest SpO_2 during sleep was calculated in each patient. OSA severity was defined by the AHI as follows: non OSA ($AHI<5$), mild OSA ($5 \leq AHI<15$), moderate OSA ($15 \leq AHI<30$) and severe OSA ($30 \leq AHI$).

Blood sample collection and measurements of serum biomarkers levels

Following overnight polysomnography, samples of peripheral venous blood were collected in the morning after an overnight fast. Serum KL-6 levels were measured by a sandwich-type electrochemiluminescence immunoassay kit (Picolumi KL-6; Sanko Junyaku, Tokyo, Japan), serum SP-D levels were measured by a sandwich-type enzyme immunoassay kit (SP-D kit Yamasa EIA II; Yamasa Shoyu, Chiba, Japan), and serum CRP levels were measured using a high sensitive assay kit (N-Assay LA CRP-S kit; Nittobo Medical, Tokyo, Japan).

Pulmonary function tests

Pulmonary function tests were performed using CHESTAC (Chest M.I. Inc., Tokyo, Japan). Residual volume (RV) and total lung capacity (TLC) were measured by the closed-circuit helium method, and diffusing capacity for carbon monoxide (DL_{CO}) was measured using a single-breath technique. Percent-predicted values were used for analyses.

Statistics

All statistical analyses were performed using StatView version 5.0 for Windows (Abacus Concepts, Berkeley, CA, USA). Continuous variables are expressed as means ± standard deviation (SD). The unpaired *t*-test was used to compare AHI levels between men and women. The significance of intergroup differences based on the severity of OSA was determined by an analysis of variance (ANOVA). When a significant difference was observed, we used the Fisher's PLSD method to identify where the differences were significant. A chi-square test was used to compare dichotomous variables. Relationships between 2 variables were analyzed by Pearson's correlation coefficient tests. The trend of serum biomarker levels across OSA groups was examined by two models. Model 1 is a linear model with serum biomarker levels as the dependent variable and with three indicator variables for mild, moderate, and severe OSA as the independent variables. We reported the β coefficients for the three OSA variables as mean differences in biomarker levels versus the non OSA group (reference). Model 2 is also a linear model wherein the indicator variables are replaced with a single ordinal variable equal to the median AHI in the mild, moderate and severe OSA groups, respectively and 0 in the non OSA group. Multiple regression analyses were performed to adjust for the confounders. A p value less than 0.05 was considered to indicate statistical significance.

Results

Relationships of clinical indices and serum biomarker levels to AHI

Patient characteristics and polysomnographic data are shown in Table 1. The study group of 170 patients was comprised of 20 non OSA, 25 mild OSA, 52 moderate OSA and 73 severe OSA patients. Significant differences were observed in sex, age, body mass index (BMI) and smoking among the groups. Serum KL-6 levels were also significantly different among the groups ($p = 0.04$), but not SP-D ($p = 0.65$) or CRP ($p = 0.53$). There were significant differences among the groups in PaO_2 and A-aDO_2.

We investigated the relationships between subjects' background, serum biomarker levels and AHI. With regard to clinical characteristics, the AHI was not significantly different between men and women ($p = 0.12$), and had significant positive correlations with BMI [r (correlation coefficient) $= 0.50$, $p < 0.001$] and smoking ($r = 0.23$, $p = 0.003$), but not with age ($r = 0.06$, $p = 0.44$). On the other hand, the AHI had a significant positive correlation with serum levels of KL-6 ($r = 0.20$, $p = 0.01$) and CRP ($r = 0.17$, $p = 0.03$), although a significant correlation was not found between the AHI and serum levels of SP-D ($r = 0.06$, $p = 0.48$). After adjustment for BMI and smoking, which were significantly associated with the AHI as mentioned above, the correlation of the AHI with serum KL-6 levels remained weak but statistically significant (β coefficient $= 0.14$, $p = 0.03$), whereas its correlation with serum CRP levels was far from significant (β coefficient $= 0.00$, $p = 0.97$).

Table 2 shows trends of serum biomarker levels across OSA groups. A significant trend for an increase in serum KL-6 levels was noted in accordance with the severity of OSA even after adjustment for BMI and smoking (β coefficient $= 0.18$, $p = 0.02$ for both Model 1 and 2), whereas no significant trend was found in serum levels of SP-D and CRP.

As to the lowest SpO_2, no significant relationships with serum levels of KL-6, SP-D and CRP were found. Regarding the inter-relationships among the three serum biomarkers examined, there was a significant correlation between serum levels of KL-6 and SP-D ($r = 0.24$, $p = 0.002$), but serum CRP levels did not correlate with either KL-6 or SP-D levels.

Relationships of pulmonary function and arterial blood gas data to serum biomarker levels

Next, to assess the clinical relevance of KL-6 and CRP, which were significantly related to AHI, we compared their relationships with pulmonary function and arterial blood gas data. After adjustment for BMI and smoking, serum KL-6 levels were significantly positively correlated with A-aDO_2 and negatively correlated with vital capacity (VC), forced vital capacity (FVC), TLC and DL_{CO} (Table 3). In contrast, serum CRP levels were significantly positively correlated with TLC and negatively correlated with forced expiratory volume in 1 s (FEV_1) (Table 3).

Discussion

We analyzed the inter-relationships of different serum biomarkers with OSA and pulmonary function. We found that, after adjustment for obesity and smoking, the serum KL-6 levels significantly correlated with the AHI, unlike serum levels of SP-D and CRP. Additionally, elevated serum KL-6 levels were significantly associated with increased A-aDO_2 and decreased VC, FVC, TLC and DL_{CO} even after adjustment for obesity and smoking, whereas elevated serum CRP levels were significantly associated with increased TLC and decreased FEV_1.

Our results indicate the significance of circulating levels of KL-6 as a marker of lung injury associated with OSA. Although Lederer et al. reported elevated circulating levels of KL-6 in some patients with OSA in comparison with controls in a study having a small sample size,[7] we expanded knowledge in this area by confirming the significant relationship between serum KL-6 levels and the severity of OSA with a relatively large number of subjects and, in addition, compared values for serum KL-6 with

Table 1 Clinical characteristics and polysomnographic data on 170 patients.

	non OSA (n = 20)	mild OSA (n = 25)	moderate OSA (n = 52)	severe OSA (n = 73)	p value
Sex (male/female)	12/8	16/9	37/15	62/11[a,c]	0.04
Age (years)	43.6 ± 17.7	56.7 ± 15.7[a]	57.5 ± 15.6[a]	57.3 ± 13.5[a]	0.003
BMI (kg/m^2)	24.8 ± 3.4	25.7 ± 4.1	25.6 ± 5.3	28.7 ± 6.1[a,b,c]	0.002
Smoking history (current/ex/never)	12/6/2	9/9/7	26/18/8	18/39/16[a,c]	0.02
Smoking (pack years)	5.4 ± 12.7	18.0 ± 23.3	21.1 ± 34.2[a]	28.3 ± 30.9[a]	0.02
Serum KL-6 (U/ml)	198.7 ± 56.0	227.2 ± 90.0	246.8 ± 117.1	285.7 ± 170.8[a]	0.04
Serum SP-D (ng/ml)	41.6 ± 26.4	48.4 ± 22.3	53.0 ± 43.7	51.9 ± 36.1	0.65
Serum CRP (mg/dl)	0.14 ± 0.27	0.20 ± 0.40	0.13 ± 0.22	0.21 ± 0.32	0.53
AHI (events/hour)	2.2 ± 1.5	9.8 ± 2.8	22.1 ± 4.3[a,b]	54.3 ± 21.6[a,b,c]	<0.0001
Lowest SpO_2 (%)	89.7 ± 6.4	84.4 ± 8.3	80.3 ± 11.3[a]	73.9 ± 9.3[a,b,c]	<0.0001
VC (% predicted)	107.3 ± 13.3	107.8 ± 19.0	113.0 ± 15.5	110.6 ± 17.4	0.46
ERV (% predicted)	82.8 ± 26.1	81.6 ± 36.9	83.1 ± 38.5	71.1 ± 35.8	0.23
FVC (% predicted)	107.7 ± 14.0	105.4 ± 19.7	111.8 ± 16.3	108.5 ± 17.9	0.46
FEV_1 (% predicted)	99.4 ± 13.6	98.9 ± 20.7	107.2 ± 15.5	106.3 ± 17.9	0.10
FRC (% predicted)	106.9 ± 24.4	103.2 ± 30.2	111.5 ± 47.9	125.4 ± 41.9	0.71
RV (% predicted)	108.4 ± 37.6	113.2 ± 38.9	104.9 ± 26.9	106.4 ± 41.2	0.81
TLC (% predicted)	95.3 ± 13.8	102.0 ± 25.9	99.3 ± 18.9	96.6 ± 15.4	0.50
DL_{CO} (% predicted)	89.4 ± 15.7	82.0 ± 17.3	81.1 ± 19.3	85.7 ± 15.1	0.21
$PaCO_2$ (kPa)	5.7 ± 0.5	5.6 ± 0.5	5.7 ± 0.5	5.6 ± 0.6	0.61
PaO_2 (kPa)	12.0 ± 1.7	11.6 ± 1.7	11.5 ± 1.4	10.9 ± 1.6[a,c]	0.01
A-aDO_2 (kPa)	0.9 ± 1.7	1.5 ± 1.6	1.3 ± 0.4	2.1 ± 1.5[a,c]	0.003

Data presented as number or mean ± SD.
[a] $p < 0.05$ versus non OSA.
[b] $p < 0.05$ versus mild OSA.
[c] $p < 0.05$ versus moderate OSA. OSA: obstructive sleep apnea; BMI: body mass index; SP-D: surfactant protein-D; CRP: C-reactive protein; AHI: apnea/hypopnea index; VC: vital capacity; ERV: expiratory reserve volume; FVC: forced vital capacity; FEV_1: forced expiratory volume in 1 s; FRC: functional residual capacity; RV: residual volume; TLC: total lung capacity; DL_{CO}: diffusing capacity for carbon monoxide; $PaCO_2$: arterial partial tension of carbon dioxide; PaO_2: arterial partial tension of oxygen; A-aDO_2: alveolar-arterial oxygen tension difference.

other potential biomarkers. Moreover, elevated KL-6 levels were also significantly associated with restrictive lung function disturbance and gas exchange derangement, which are characteristic features in lung injury. Lederer et al. speculated that the possible mechanisms whereby OSA leads to lung injury include chronic oxidative stress associated with repeated intermittent hypoxia and reoxygenation and mechanical stretch caused by dynamic changes in intrathoracic pressure.[7] In addition to these factors, snoring-induced vibratory force might be a candidate as another factor causing lung injury.[19] Although both comorbid obesity and smoking exposure could affect plasma cytokine levels[20] or the subjects' lung diffusion capacity,[21,22] we showed that even after adjustment for these confounders the association between KL-6, pulmonary function impairment and OSA remained significant, indicating the possible pathogenetic role of OSA itself in lung injury.

KL-6 is a well-known biomarker for the diagnosis of IPF and determination of the severity of this condition.[23,24]

Table 2 Trends of serum biomarker levels across OSA groups.

	Model 1		Model 2	
	Unadjusted	Adjusted[a]	Unadjusted	Adjusted[a]
Serum KL-6 (U/ml)	β = 0.22	β = 0.18	β = 0.22	β = 0.18
	p = 0.004	p = 0.02	p = 0.004	p = 0.02
Serum SP-D (ng/ml)	β = 0.08	β = 0.04	β = 0.07	β = 0.02
	p = 0.28	p = 0.67	p = 0.39	p = 0.80
Serum CRP (mg/dl)	β = 0.06	β = −0.02	β = 0.08	β = −0.01
	p = 0.41	p = 0.84	p = 0.32	p = 0.88

Model 1: Linear model with three indicator variables for mild, moderate, and severe OSA as independent variables. Model 2: Linear model in which indicator variables were replaced with a single ordinal variable equal to the median AHI in the mild, moderate and severe OSA groups, respectively, and 0 in the non OSA group. OSA: obstructive sleep apnea; SP-D: surfactant protein-D; CRP: C-reactive protein.
[a] Adjusted for body mass index and smoking.

Table 3 Relationships between serum biomarker levels and pulmonary function and arterial blood gas data.

	Serum KL-6 (U/ml)		Serum CRP (mg/dl)	
	β coefficient	p value	β coefficient	p value
VC (% predicted)	−0.20	0.01	−0.08	0.24
ERV (% predicted)	−0.15	0.07	−0.03	0.75
FVC (% predicted)	−0.22	0.003	−0.11	0.14
FEV_1 (% predicted)	−0.11	0.17	−0.19	0.008
FRC (% predicted)	0.15	0.11	−0.02	0.79
RV (% predicted)	0.05	0.53	0.12	0.11
TLC (% predicted)	−0.14	0.049	0.18	0.01
DL_{CO} (% predicted)	−0.22	0.005	−0.14	0.06
$PaCO_2$ (kPa)	−0.12	0.12	0.10	0.16
PaO_2 (kPa)	−0.13	0.11	−0.11	0.16
A-aDO_2 (kPa)	0.18	0.02	0.06	0.45

These analyses were adjusted by body mass index and smoking. VC: vital capacity; ERV: expiratory reserve volume; FVC: forced vital capacity; FEV_1: forced expiratory volume in 1 s; FRC: functional residual capacity; RV: residual volume; TLC: total lung capacity; DL_{CO}: diffusing capacity for carbon monoxide; $PaCO_2$: arterial partial tension of carbon dioxide; PaO_2: arterial partial tension of oxygen; A-aDO_2: alveolar-arterial oxygen tension difference.

Although the pathophysiological link between IPF and OSA remains unclear, as a new topic in the field of IPF, recent studies have reported a high prevalence of OSA in IPF patients.[16,25] Our findings may partially explain potential mechanisms underlying this association and also provide a warning that their combination as a comorbid condition may additively worsen lung injury.

Serum levels of CRP did not correlate with the severity of OSA independently of BMI in our study, which is consistent with some reports.[26,27] Obesity was shown to be associated with chronic low-grade inflammation as indicated by raised serum CRP levels.[28] Considering that CRP reflects obesity-related inflammation, it could be anticipated that CRP might have an association with reduced lung volume due to obesity, particularly visceral adiposity. However, notably, we found that elevated CRP levels were significantly associated with worsened airflow limitation and increased lung volume independently of obesity and smoking, as contrasted with the significant relationship between KL-6 and restrictive defects. Increased levels of CRP also have been reported in obstructive and restrictive lung disease,[29] and were shown to be correlated with lower levels of FEV_1[30–32] and a decline in FEV_1.[33] Moreover, a recent large-scale population-based study showed that abdominal obesity was positively related to both obstructive and restrictive ventilatory patterns regardless of BMI.[34] Thus, the inter-relationships among OSA, pulmonary function, obesity and inflammatory markers are complicated, and further studies are needed.

Contrary to our hypothesis, unlike KL-6, SP-D was not significantly associated with the severity of OSA, although both are mainly produced by alveolar type II cells. Leakage of these markers into the bloodstream may be dependent on an alteration of production by alveolar type II cells and, in addition, on the intensity, extent, and type of injuries that precipitate the increase in alveolar wall permeability.[24] Thus, the magnitude of lung injury in patients with OSA might be too subtle to increase the production of SP-D by alveolar type II cells, although we did not assess the local concentrations of SP-D in lung compartments. SP-D was recently reported to be a promising lung-specific biomarker in COPD.[10] However, results of previous studies suggested that KL-6 was a more discriminative biomarker than SP-D in IPF and collagen vascular disease-associated interstitial pneumonitis,[24] idiopathic pulmonary alveolar proteinosis[35] or sarcoidosis.[36] Madsen et al. reported that SP-D was widely distributed in epithelial cells in a variety of tissues and was not restricted to the respiratory system.[37] Only a weak, though significant, relationship between serum levels of KL-6 and SP-D in the present study indicates that the blood level of these two cytokines may not necessarily reflect the same pathological state of the disease. Thus, although KL-6 appears to be superior to SP-D in evaluating subclinical lung injury associated with OSA, further study is needed to explain this discrepancy.

OSA is associated with significant morbidity and mortality. Analyses of biomarkers in OSA have been extensively performed in relation to its cardiovascular effects through systemic inflammation.[12] However, as well as systemic inflammation, local inflammation or injury is also implicated in the pathophysiology of OSA.[38,39] Local inflammation or injury has been assessed by surgical specimens, exhaled breath condensate (EBC), induced sputum, exhaled breath and oral air,[38,39] but more studies with a lung-specific biomarker in OSA are necessary for future use of such biomarkers in clinical practice. A recent study has also reported that the combination of two biomarkers, SP-D (lung epithelial barrier injury) and interleukin-8 (inflammation and neutrophil chemotaxis), had significant prognostic value, reflecting the two important pathogenetic pathways of acute lung injury.[40] Thus, KL-6 in association with a systemic biomarker such as CRP might provide complementarily useful information in assessing OSA.

In our study, there was a significant positive relationship between AHI and smoking. Airway inflammation and damage due to cigarette smoke could alter the mechanical and neural properties of the upper airway and increase its collapsibility during sleep, which may be related to sleep apnea.[41]

The prevalence of OSA in our population was high (88.2%). Since all participants in our study were referred to

our sleep unit with suspicious symptoms, there was a high clinical probability of OSA among these patients. Actually, the diagnostic rates in some other sleep laboratories were comparable to ours.[42–44]

The present study has some limitations. First, as we did not directly assess local expressions of KL-6 in the lung and alveolar wall permeability in OSA patients, our results cannot clearly establish the presence of lung injury in OSA. Measurements of KL-6, albumin concentration or cell count in bronchoalveolar lavage fluid, EBC or induced sputum would provide additional information and supporting evidence for our suggestions regarding the implications of these results. Second, as we did not assess serum biomarker levels after treatment of OSA, we could not confirm the specific association between OSA and serum biomarkers. Third, as the values of AHI and biomarkers tended to be skewed, we tried to transform them logarithmically. However, in 57 patients the CRP values could not be transformed logarithmically (CRP value was '0'). We then made calculations using absolute values. However, significance of the result between KL-6 and AHI remained even after logarithmic transformation ($r = 0.20$, $p = 0.01$).

In summary, serum levels of KL-6 but not SP-D were correlated with subclinical lung injury associated with OSA independently of obesity or smoking, and KL-6 could be a potential candidate as a lung-specific biomarker in OSA. KL-6 values may pathologically reflect epithelial and endothelial injury in the alveolus and pulmonary function impairment in OSA. This is in contrast to CRP, which is a well-studied systemic biomarker and may preferably cause an obstructive defect. A combination of two different types of biomarkers might be complementary and be superior to each biomarker alone from a pathogenesis perspective.

Conflict of interest disclosure

Kazuo Chin received Grants from the Japanese Ministry of Education, Culture, Sports, Science and Technology (nos. 20590921 and 22590860), Respiratory Failure Research Group and Health Science Research Grants (Comprehensive Research on Life-Style Related Diseases including Cardiovascular Diseases and Diabetes Mellitus: nos. 22110201 and 22111201) from the Ministry of Health, Labor and Welfare of Japan, and the Japan Vascular Disease Research Foundation.

References

1. Arnardottir ES, Mackiewicz M, Gislason T, Teff KL, Pack AI. Molecular signatures of obstructive sleep apnea in adults: a review and perspective. *Sleep* 2009;**32**:447–70.
2. Cochrane CG, Spragg R, Revak SD. Pathogenesis of the adult respiratory distress syndrome. Evidence of oxidant activity in bronchoalveolar lavage fluid. *J Clin Invest* 1983;**71**:754–61.
3. Kiefmann R, Rifkind JM, Nagababu E, Bhattacharya J. Red blood cells induce hypoxic lung inflammation. *Blood* 2008;**111**: 5205–14.
4. Kohno N, Inoue Y, Hamada H, et al. Difference in sero-diagnostic values among KL-6-associated mucins classified as cluster 9. *Int J Cancer Suppl* 1994;**8**:81–3.
5. Ishizaka A, Matsuda T, Albertine KH, et al. Elevation of KL-6, a lung epithelial cell marker, in plasma and epithelial lining fluid in acute respiratory distress syndrome. *Am J Physiol Lung Cell Mol Physiol* 2004;**286**:L1088–94.
6. Sato H, Callister ME, Mumby S, et al. KL-6 levels are elevated in plasma from patients with acute respiratory distress syndrome. *Eur Respir J* 2004;**23**:142–5.
7. Lederer DJ, Jelic S, Basner RC, Ishizaka A, Bhattacharya J. Circulating KL-6, a biomarker of lung injury, in obstructive sleep apnoea. *Eur Respir J* 2009;**33**:793–6.
8. Eisner MD, Parsons P, Matthay MA, Ware L, Greene K. Plasma surfactant protein levels and clinical outcomes in patients with acute lung injury. *Thorax* 2003;**58**:983–8.
9. Cheng IW, Ware LB, Greene KE, Nuckton TJ, Eisner MD, Matthay MA. Prognostic value of surfactant proteins A and D in patients with acute lung injury. *Crit Care Med* 2003;**31**:20–7.
10. Sin DD, Pahlavan PS, Man SF. Surfactant protein D: a lung specific biomarker in COPD? *Ther Adv Respir Dis* 2008;**2**:65–74.
11. Sin DD, Man SF, Marciniuk DD, et al. The effects of fluticasone with or without salmeterol on systemic biomarkers of inflammation in chronic obstructive pulmonary disease. *Am J Respir Crit Care Med* 2008;**177**:1207–14.
12. Ryan S, Taylor CT, McNicholas WT. Systemic inflammation: a key factor in the pathogenesis of cardiovascular complications in obstructive sleep apnoea syndrome? *Thorax* 2009;**64**: 631–6.
13. Chan KK, Ing AJ, Laks L, Cossa G, Rogers P, Birring SS. Chronic cough in patients with sleep-disordered breathing. *Eur Respir J* 2010;**35**:368–72.
14. Shore SA. Obesity and asthma: possible mechanisms. *J Allergy Clin Immunol* 2008;**121**:1087–93.
15. Marin JM, Soriano JB, Carrizo SJ, Boldova A, Celli BR. Outcomes in patients with chronic obstructive pulmonary disease and obstructive sleep apnea: the overlap syndrome. *Am J Respir Crit Care Med* 2010;**182**:325–31.
16. Mermigkis C, Stagaki E, Tryfon S, et al. How common is sleep-disordered breathing in patients with idiopathic pulmonary fibrosis? *Sleep Breath* 2010;**14**:387–90.
17. Rechtschaffen A, Kales A. *A Manual of Standardized Terminology, techniques and Scoring system for sleep stages of human subjects*. Washington, DC: National Institutes of Health; 1968.
18. Iber C, Ancoli-Israel S, Chesson A, Quan S. *The AASM Manual for the Scoring of sleep and associated Events: Rules, Terminology and Technical Specifications*. Westchester, IL, USA: American Academy of Sleep Medicine; 2007.
19. Puig F, Rico F, Almendros I, Montserrat JM, Navajas D, Farre R. Vibration enhances interleukin-8 release in a cell model of snoring-induced airway inflammation. *Sleep* 2005;**28**:1312–6.
20. Stapleton RD, Dixon AE, Parsons PE, Ware LB, Suratt BT. The association between BMI and plasma cytokine levels in patients with acute lung injury. *Chest* 2010;**138**:568–77.
21. Collard P, Wilputte JY, Aubert G, Rodenstein DO, Frans A. The single-breath diffusing capacity for carbon monoxide in obstructive sleep apnea and obesity. *Chest* 1996;**110**:1189–93.
22. Rizzi M, Sergi M, Andreoli A, Pecis M, Bruschi C, Fanfulla F. Environmental tobacco smoke may induce early lung damage in healthy male adolescents. *Chest* 2004;**125**:1387–93.
23. Yokoyama A, Kohno N, Hamada H, et al. Circulating KL-6 predicts the outcome of rapidly progressive idiopathic pulmonary fibrosis. *Am J Respir Crit Care Med* 1998;**158**:1680–4.
24. Ohnishi H, Yokoyama A, Kondo K, et al. Comparative study of KL-6, surfactant protein-A, surfactant protein-D, and monocyte chemoattractant protein-1 as serum markers for interstitial lung diseases. *Am J Respir Crit Care Med* 2002;**165**: 378–81.
25. Lancaster LH, Mason WR, Parnell JA, et al. Obstructive sleep apnea is common in idiopathic pulmonary fibrosis. *Chest* 2009; **136**:772–8.
26. Taheri S, Austin D, Lin L, Nieto FJ, Young T, Mignot E. Correlates of serum C-reactive protein (CRP)—no association with

sleep duration or sleep disordered breathing. *Sleep* 2007;**30**: 991–6.
27. Ryan S, Nolan GM, Hannigan E, Cunningham S, Taylor C, McNicholas WT. Cardiovascular risk markers in obstructive sleep apnoea syndrome and correlation with obesity. *Thorax* 2007;**62**:509–14.
28. Visser M, Bouter LM, McQuillan GM, Wener MH, Harris TB. Elevated C-reactive protein levels in overweight and obese adults. *JAMA* 1999;**282**:2131–5.
29. Mannino DM, Ford ES, Redd SC. Obstructive and restrictive lung disease and markers of inflammation: data from the Third National Health and Nutrition Examination. *Am J Med* 2003; **114**:758–62.
30. Takemura M, Matsumoto H, Niimi A, et al. High sensitivity C-reactive protein in asthma. *Eur Respir J* 2006;**27**:908–12.
31. Gan WQ, Man SF, Sin DD. The interactions between cigarette smoking and reduced lung function on systemic inflammation. *Chest* 2005;**127**:558–64.
32. Walter RE, Wilk JB, Larson MG, et al. Systemic inflammation and COPD: the Framingham Heart study. *Chest* 2008;**133**:19–25.
33. Shaaban R, Kony S, Driss F, et al. Change in C-reactive protein levels and FEV_1 decline: a longitudinal population-based study. *Respir Med* 2006;**100**:2112–20.
34. Leone N, Courbon D, Thomas F, et al. Lung function impairment and metabolic syndrome: the critical role of abdominal obesity. *Am J Respir Crit Care Med* 2009;**179**:509–16.
35. Lin FC, Chen YC, Chang SC. Clinical importance of bronchoalveolar lavage fluid and blood cytokines, surfactant protein D, and Kerbs von Lungren 6 antigen in idiopathic pulmonary alveolar proteinosis. *Mayo Clin Proc* 2008;**83**: 1344–9.
36. Janssen R, Sato H, Grutters JC, et al. Study of Clara cell 16, KL-6, and surfactant protein-D in serum as disease markers in pulmonary sarcoidosis. *Chest* 2003;**124**:2119–25.
37. Madsen J, Kliem A, Tornoe I, Skjodt K, Koch C, Holmskov U. Localization of lung surfactant protein D on mucosal surfaces in human tissues. *J Immunol* 2000;**164**:5866–70.
38. Bergeron C, Kimoff J, Hamid Q. Obstructive sleep apnea syndrome and inflammation. *J Allergy Clin Immunol* 2005;**116**: 1393–6.
39. Culla B, Guida G, Brussino L, et al. Increased oral nitric oxide in obstructive sleep apnoea. *Respir Med* 2010;**104**:316–20.
40. Ware LB, Koyama T, Billheimer DD, et al. Prognostic and pathogenetic value of combining clinical and biochemical indices in patients with acute lung injury. *Chest* 2010;**137**: 288–96.
41. Punjabi NM. The epidemiology of adult obstructive sleep apnea. *Proc Am Thorac Soc* 2008;**5**:136–43.
42. Botros N, Concato J, Mohsenin V, Selim B, Doctor K, Yaggi HK. Obstructive sleep apnea as a risk factor for type 2 diabetes. *Am J Med* 2009;**122**:1122–7.
43. Kemmer H, Mathes AM, Dilk O, Gröschel A, Grass C, Stöckle M. Obstructive sleep apnea syndrome is associated with overactive bladder and urgency incontinence in men. *Sleep* 2009; **32**:271–5.
44. Fleischmann G, Fillafer G, Matterer H, Skrabal F, Kotanko P. Prevalence of chronic kidney disease in patients with suspected sleep apnoea. *Nephrol Dial Transplant* 2010;**25**:181–6.

BMC Pulmonary Medicine

RESEARCH ARTICLE Open Access

Efficacy and safety of inhaled formoterol 4.5 and 9 μg twice daily in Japanese and European COPD patients: Phase III study results

Miron A Bogdan[1*], Hisamichi Aizawa[2], Yoshinosuke Fukuchi[3], Michiaki Mishima[4], Masaharu Nishimura[5] and Masakazu Ichinose[6]

Abstract

Background: This study evaluated the efficacy and safety of the long-acting β_2-agonist formoterol in patients with moderate-to-severe COPD.

Methods: This double-blind, placebo-controlled, parallel-group, multinational phase III study randomized patients ≥ 40 years of age with moderate-to-severe COPD to inhaled formoterol 4.5 or 9 μg twice daily (bid) via Turbuhaler® or placebo for 12 weeks. Salbutamol 100 μg/actuation via pMDI was permitted as reliever medication. The primary outcome variable was change (ratio) from baseline to treatment period in FEV_1 60-min post-dose.

Results: 613 patients received treatment (formoterol 4.5 μg n = 206; 9 μg n = 199; placebo n = 208); 539 (87.9%) male; 324 (52.9%) Japanese and 289 (47.1%) European. End of study increases in FEV_1 60-min post-dose were significantly greater ($p < 0.001$ for both) with formoterol 4.5 and 9 μg bid (113% of baseline for both) than with placebo, as were all secondary outcome measures. The proportion of patients with an improvement in St George's Respiratory Questionnaire score of ≥ 4 was 50.2% for formoterol 4.5 μg ($p = 0.0682$ vs. placebo), 59.2% ($p = 0.0004$) for 9 μg, and 41.3% for placebo. Reduction in reliever medication use was significantly greater with formoterol vs. placebo (9 μg: -0.548, $p < 0.001$; 4.5 μg: -0.274, $p = 0.027$), with 9 μg being significantly superior to 4.5 μg (-0.274, $p = 0.029$). Formoterol was well tolerated with the incidence and type of adverse events not being different for the three groups.

Conclusions: Formoterol 4.5 μg and 9 μg bid was effective and well tolerated in patients with COPD; there was no difference between formoterol doses for the primary endpoint; however, an added value of formoterol 9 μg over 4.5 μg bid was observed for some secondary endpoints.

Trial registration: NCT00628862 (ClinicalTrials.gov); D5122C00001 (AstraZeneca Study code).

Background

Chronic obstructive pulmonary disease (COPD) is a chronic, progressive respiratory disease that follows a course of declining lung function and markedly impaired quality of life, and places patients at a significantly increased risk of premature death [1,2]. The pulmonary component of the disease is characterized by airflow obstruction that is not fully reversible and is associated with symptoms of breathlessness, cough, and reduced physical exercise capacity resulting from inflammatory and destructive changes in the lungs. Exacerbations are common, particularly in severe stages of the disease, and frequently lead to hospitalization and can be life-threatening.

Bronchodilator therapy is the mainstay of pharmacotherapy for COPD with treatment with short-acting bronchodilators being recommended in patients with mild COPD, while long-acting β_2-agonists (LABAs) and anticholinergics are added for patients with moderate to severe COPD. Despite an underlying inflammatory component to the disease, the use of LABAs for the treatment of COPD is generally advocated without concomitant inhaled corticosteroid (ICS) therapy. ICS

* Correspondence: miron.a.bogdan@gmail.com
[1]Clinica Medic Or, Calea Vitan no 106, Postcode 031298, Bucharest, Romania
Full list of author information is available at the end of the article